The hidden sunrise in the energy-energy correlator

Matthew D. Schwartz[1, 2, *] and Xiaoyuan Zhang[2, 3, †]

[1] *Department of Physics, Harvard University, Cambridge, MA 02138, USA*

[2] *The NSF AI Institute for Artificial Intelligence and Fundamental Interactions*

[3] *Center for Theoretical Physics – a Leinweber Institute, Massachusetts Institute of Technology, Cambridge, MA 02139, USA*

(Dated: October 1, 2026)

The energy-energy correlator (EEC) is one of a handful of collider observables that can be computed analytically to high order. As an energy-weighted cross section, it exposes features of quantum field theory that scattering amplitudes do not, and it can be compared directly to data. Similar to scattering amplitudes, the analytic expressions require special functions beyond polylogarithms. In Ref. [1], EEC is computed to next-to-next-to-leading order (NNLO) for $\mathcal{N} = 4$ super Yang-Mills (SYM) theory, and the result is expressed in terms of both harmonic polylogarithms (HPLs) and one two-fold integral, which contains elliptic curves. In this work, we report a complete result including the remaining elliptic sector, which is closely related to the sunrise Feynman integrals. We find the j-invariants of the EEC and the sunrise agree identically under a Möbius map, and thus the elliptic sector in EEC lives on the $\Gamma_1(6)$ modular curve of the sunrise integral. We then express the answer with iterated Eisenstein integrals, which can be evaluated to high precision quickly. The analytic form also allows us a first study on the EEC Landau bootstrap, and the understanding of its function space in $\mathcal{N} = 4$ SYM offers a concrete handle on the elliptic sector of the EEC in QCD.

* schwartz@g.harvard.edu

† xyz2@mit.edu

CONTENTS

I. Introduction 3

II. EEC at NNLO and partial fraction 5

III. The elliptic curve and the sunrise 9

A. Elliptic curve in EEC 9

B. Further decomposition of F_{R_2} 12

IV. Analytic results 13

A. The polylogarithmic sector 14

B. The elliptic sector 15

1. Solving the system 15

2. Iterated Eisenstein integrals 18

3. Numerical evaluations 20

C. Final result 21

V. A first look at EEC bootstrap 25

A. Alphabet and function space 26

B. Rational coefficients ansatz 29

C. Physical and numerical constraints 31

D. Results 33

1. LO and NLO bootstrap 33

2. NNLO bootstrap 36

VI. Conclusions 37

Acknowledgments 39

A. Function classes and conventions 39

B. The sources of the elliptic system 40

References 43

I. INTRODUCTION

The energy-energy correlator (EEC) measures the energy deposited in two calorimeter cells at an angular separation χ and probes correlations in energy flow in a scattering event. Proposed in the 1970s [2–5], EEC has been used as an event-shape observable at colliders and to study different aspects of quantum chromodynamics (QCD). The fact that EEC is infrared finite, jet-algorithm free, and soft-divergence suppressed makes it among the simplest observables in perturbative QCD. Such simplicity allows one to study its analytic structure and geometry, and improve our understanding of quantum field theories.

In perturbation theory, QCD and $\mathcal{N}=4$ super Yang-Mills (SYM) theory share many common features, and the latter is often used as a simpler model for testing techniques. EEC has been computed to next-to-next-to-leading order (NNLO) in $\mathcal{N}=4$ SYM [1, 6], and to NLO in both e^+e^- annihilation and hadronic Higgs decays [7–9]. The availability of fixed-order data allows one to study the singular limits of EEC, namely the collinear limit ($\chi \to 0$) and back-to-back limit ($\chi \to \pi$), and provides the ingredients for large logarithmic resummation in effective field theories. Specifically, EEC has been resummed to next-to-next-to-leading logarithmic (NNLL) order in the collinear limit [10–12] and N^{4}LL in the back-to-back limit [13–21]. These results have been applied to QCD studies, for example, the measurement of the strong coupling constant [16]. Interest in the EEC has grown with the development of multi-point energy correlators. In Refs. [22, 23], EEC is generalized to N-point energy correlators, where one weights the differential cross-section by energy deposited from more than two detectors and measures the angles between any pair among them. The differential three-point correlator has been calculated at LO in $\mathcal{N}=4$ SYM [24] and QCD [25, 26]. The four-point correlator has been computed to LO only in $\mathcal{N}=4$ SYM and under the collinear limit [27], while the mathematical structure for generic angles is explored in Ref. [28].

Feynman integrals generally give rise to iterative functions like polylogarithms. For EEC up to NLO and three-point correlator at LO, which is of order $\mathcal{O}(g_{\rm YM}^4)$ in the coupling $g_{\rm YM}$, the results can be expressed in terms of generalized polylogarithms up to weight 3. Starting from EEC at NNLO or four-point correlator at LO, polylogarithms run out and elliptic functions appear. Similar behavior is observed in scattering amplitudes and loop integrals. The first elliptic Feynman integral is the two-loop equal-mass sunrise diagram [29–33]. For higher-loop integrals or observables like $N \geq 4$-point energy correlators, richer geometries appear and the analytic results require special functions beyond elliptic ones. Unlike polylogarithms, where the function space can be well organized using Symbol [34] and transcendental weights, and they can be evaluated fast using GiNaC [35] or other

packages [36, 37], elliptic functions and beyond are still open problems. On one hand, there is no well-developed method to calculate Feynman integrals with elliptic curves and systematically express the result in terms of universal basis functions, while for polylogarithmic integrals, one can derive canonical differential equations and write the results with generalized polylogarithms (GPLs). On the other hand, it is difficult to numerically evaluate elliptic functions and beyond to high precision, though iterated integrals of modular forms and elliptic multiple polylogarithms have been implemented in GiNaC [38, 39].

Our understanding of polylogarithmic Feynman integrals has fostered the development of perturbative bootstrap programs. To the best of our knowledge, these programs fall into two categories: amplitude bootstrap and Landau bootstrap. The amplitude bootstrap [40–49] uses the properties of scattering amplitudes like unitarity and supersymmetry to constrain the symbol basis and determine the final expression. Landau bootstrap (also called Feynman integral bootstrap) [50–54] focuses on the leading singularities of Feynman integrals and constructs the symbol basis from their analytic properties. In both cases, one writes down all possible integrable symbols up to certain weights, lifts them to polylogarithmic functions and uses the constraints to determine the coefficients. Very recently, we also developed the analytic regression method [55], which can help bypass some consistency constraints. These bootstrap methods have also been applied to individual elliptic Feynman integrals [56], but so far, not to a collider observable with an elliptic sector. EEC at NNLO is a natural place to initiate such a bootstrap program.

In this work, we study the remaining two-fold integral in NNLO EEC for $\mathcal{N}=4$ SYM theory. Guided by Galois symmetry [57], we can perform partial fraction decomposition on the integrand and separate the elliptic sector from the polylogarithmic sector. The polylogarithmic sector can be integrated directly and the result is HPL. They are then combined with the existing HPL contribution in Ref. [1]. For the elliptic sector, we identify a single elliptic curve, which turns out to be the sunrise curve, and write the analytic expression with iterated integrals of $\Gamma_1(6)$ Eisenstein forms [58–61]. The iterated Eisenstein integrals are polynomials in $\log q$ whose coefficients are q-series with rational coefficients, and can be evaluated to high precision. We implement their evaluation as truncated q-series, the method of Refs. [38, 58], and obtain the NNLO distribution to high precision within seconds. At the same time, the analytic form gives a first look at the EEC bootstrap program. At LO and NLO [1, 6], the function space is polylogarithmic and well organized using the EEC alphabet. Explicitly, one can write down all potential symbols with entries from the alphabet and lift to polylogarithmic functions using the integrability condition. At NNLO, the polylogarithmic sector inherits an increase in transcendental weight, and the same idea generalizes

to the elliptic sector. The elliptic letters can be identified from the underlying curves and the Eisenstein integral tower can be generated in a similar way. In both cases, we multiply the function basis by unknown rational coefficients, which are then determined by consistency conditions and numerical data.

The paper is organized as follows. In Sec. II, we review the definition of EEC and the NNLO result of Ref. [1], and perform the partial fraction that separates the remaining two-fold integral into a reducible piece F_{red_1} and two irreducible pieces F_{K_1} and F_{R_2}. In Sec. III, we show that the two irreducible pieces live on the same elliptic curve, which is the curve of the equal-mass sunrise integral, derive the differential system they satisfy, and show that their difference Δ is polylogarithmic. In Sec. IV, we provide the analytic expression of EEC at NNLO. We express the polylogarithmic part in terms of HPLs, and write the elliptic part as iterated Eisenstein integrals. In Sec. V, we analyze the alphabet and function space of EEC and initialize the perturbative EEC bootstrap program. We conclude in Sec. VI.

II. EEC AT NNLO AND PARTIAL FRACTION

In this section, we review the definition of EEC and summarize the NNLO calculation in Ref. [1]. Introducing the energy flow operator in terms of stress-energy tensor $T_{\mu\nu}$ along the direction $\vec{n}$ [62–65],

$$\mathcal{E}(\vec{n}) \;=\; \int_{-\infty}^{\infty} d\tau \;\lim_{r\to\infty} r^2\, n^i\, T_{0i}(t=\tau+r,\, r\vec{n}), \tag{1}$$

EEC is defined as a correlation function

$$\frac{d\sigma}{d\zeta} = \int d\Omega_{\vec{n}_1} d\Omega_{\vec{n}_2}\, \delta\left(\zeta - \frac{1-\vec{n}_1\cdot\vec{n}_2}{2}\right) \times \frac{\int d^4x e^{iq\cdot x}\langle 0|\mathcal{O}^\dagger(x)\mathcal{E}(\vec{n}_1)\mathcal{E}(\vec{n}_2)\mathcal{O}(0)|0\rangle}{Q^2\int d^4x e^{iq\cdot x}\langle 0|\mathcal{O}^\dagger(x)\mathcal{O}(0)|0\rangle}\,, \tag{2}$$

where $\mathcal{O}$ is the source operator in the underlying theory and we introduce the angular notation $\zeta = (1-\cos\chi)/2$. Under this variable, collinear limit ($\chi\to 0$) corresponds to $\zeta\to 0$ and back-to-back limit ($\chi\to\pi$) gives $\zeta\to 1$. In perturbation theory, EEC can also be defined as an energy-weighted cross-section,

$$\frac{d\sigma}{d\zeta} = \sum_{ij}\int d\text{LIPS}\,|\mathcal{M}|^2\,\frac{E_iE_j}{Q^2}\,\delta\left(\zeta - \frac{1-\cos\theta_{ij}}{2}\right)\,, \tag{3}$$

where dLIPS is the Lorentz-invariant phase space, $|\mathcal{M}|^2$ is the matrix element square and i,j run over all final-state particles. In terms of calculations, it is usually more convenient to use the operator definition in Eq. (2) for $\mathcal{N}=4$ SYM theory, where more conformal field theory tools are developed, and the cross-section definition in Eq. (3) for QCD processes.

In Ref. [1], the EEC in $\mathcal{N}=4$ SYM is computed to NNLO, and the result is reduced to HPLs [66] (for a review of convention, see App. A) of weight up to five plus a single unevaluated piece. Following the notation in Ref. [1], the normalized EEC is written as

$$F(\zeta) = 2\zeta^2(1-\zeta) \times \frac{d\sigma}{d\zeta} = aF_{\rm LO}(\zeta) + a^2 F_{\rm NLO}(\zeta) + a^3 F_{\rm NNLO}(\zeta) + \cdots\,, \quad a \equiv \frac{N_c g_{\rm YM}^2}{4\pi^2}\,, \tag{4}$$

with a the coupling in $\mathcal{N}=4$ SYM. The NNLO result is then expressed as

$$F_{\rm NNLO}(\zeta) \;=\; F_{\rm HPL}(\zeta) \;+\; F_R(\zeta)\,, \tag{5}$$

where $F_{\rm HPL}(\zeta)$ is an expression of weight-≤ 5 HPL with alphabet $\{\zeta, 1-\zeta, (1-\sqrt{\zeta})/(1+\sqrt{\zeta})\}$, and $F_R(\zeta)$ is a finite two-fold integral. Explicitly, the latter term can be written as

$$F_R(\zeta) = \int_0^1 \mathrm{d}\bar{z} \int_0^{\bar{z}} \mathrm{d}t\, \frac{\zeta-1}{t(\zeta-\bar{z})+(1-\zeta)\bar{z}} \left[R_1 P_1 + R_2 P_2\right], \tag{6}$$

where $R_{1,2}$ are the rational coefficients,

$$R_1(z,\bar{z}) = \frac{z\bar{z}}{1-z-\bar{z}}\,, \qquad R_2(z,\bar{z}) = \frac{z^2\bar{z}}{(1-z)^2(1-z\bar{z})}\,, \tag{7}$$

and $P_{1,2}$ are also HPL expressions,

$$\begin{aligned}
P_1(z,\bar{z}) =& -\frac{1}{8} H_0(-z)^2 H_1(z) + \frac{1}{8} H_0(-z)^2 H_1(1-\bar{z}) + \frac{1}{4} H_0(-z) H_1(z) H_1(\bar{z}) \\
&- \frac{1}{4} H_0(-z) H_1(1-\bar{z}) H_1(\bar{z}) + \frac{1}{4} H_1(z) H_1(1-\bar{z}) H_1(\bar{z}) + \frac{1}{2} H_0(-z) H_2(z) \\
&- \frac{1}{4} H_1(\bar{z}) H_2(z) - \frac{1}{2} H_0(-z) H_2(1-\bar{z}) + \frac{1}{4} H_1(z) H_2(1-\bar{z}) + \frac{1}{4} H_1(\bar{z}) H_2(1-\bar{z}) \\
&- \frac{3}{4} H_3(z) + \frac{3}{4} H_3(1-\bar{z}) - \frac{1}{4} H_1(1-\bar{z}) H_{1,1}(z) - \frac{1}{4} H_1(\bar{z}) H_{1,1}(z) \\
&+ \frac{1}{4} H_1(z) H_{1,1}(1-\bar{z}) - \frac{1}{4} H_1(\bar{z}) H_{1,1}(1-\bar{z}) - \frac{1}{4} H_{1,2}(1-\bar{z}) - \frac{1}{4} H_{2,1}(z) \\
&- \frac{1}{4} H_{2,1}(1-\bar{z}) + \frac{1}{4} H_{1,1,1}(z) - \frac{1}{4} H_{1,1,1}(1-\bar{z})\,, \\
P_2(z,\bar{z}) =& \frac{1}{6}\pi^2 H_0(-z) + \frac{1}{12}\pi^2 H_1(z) + \frac{1}{4} H_0(-z)^2 H_1(z) - \frac{1}{12}\pi^2 H_1(1-\bar{z}) + \frac{1}{4} H_0(-z)^2 H_1(1-\bar{z}) \\
&+ \frac{1}{2} H_0(-z) H_1(z) H_1(1-\bar{z}) - \frac{1}{12}\pi^2 H_1(\bar{z}) - \frac{1}{4} H_0(-z)^2 H_1(\bar{z}) \\
&+ \frac{1}{2} H_0(-z) H_1(1-\bar{z}) H_1(\bar{z}) + H_1(z) H_1(1-\bar{z}) H_1(\bar{z}) - H_0(-z) H_2(z) - H_1(\bar{z}) H_2(z) \\
&+ H_0(-z) H_2(1-\bar{z}) + H_1(z) H_2(1-\bar{z}) + H_1(\bar{z}) H_2(1-\bar{z}) + 2 H_3(z) + 2 H_3(1-\bar{z}) \\
&- \frac{1}{2} H_1(z) H_{1,1}(1-\bar{z}) + \frac{1}{2} H_1(\bar{z}) H_{1,1}(1-\bar{z}) + H_{1,2}(z) - \frac{1}{2} H_{1,1,1}(1-\bar{z})\,.
\end{aligned} \tag{8}$$

Since $P_{1,2}$ carry weight three and each of the two integrations raises the weight by one, $F_R(\zeta)$ also reaches weight five. Note that we have traded z for the integration variable t,

$$z = \frac{\zeta\, t\,(t-\bar{z})}{t(\zeta-\bar{z})+(1-\zeta)\bar{z}}\,, \tag{9}$$

so that $z \leq 0$ throughout the integration region $0 < t < \bar{z} < 1$.

From now on, we will focus on the remaining two-fold integral $F_R(\zeta)$. To separate the polylogarithmic part from the elliptic sector in $F_R(\zeta)$, we first perform the partial fraction for the rational coefficients. For convenience, we further rescale the integration variable $x = t/\bar{z} \in [0,1]$, which maps the triangle $0 < t < \bar{z} < 1$ onto the unit square, so that the inner integration boundary does not depend on the outer variable $\bar{z}$. With the new variable, we can define $D = (\zeta - \bar{z})\, x + (1-\zeta)$ and Eq. (9) becomes $z = \zeta\bar{z}\, x(x-1)/D$. The remaining integral $F_R(\zeta)$ involves D together with three quadratics in x,

$$D_j(x) = a_j\, x^2 + (\zeta - \bar{z} + c_j)\, x + e_j\,, \qquad j = 0,1,2\,, \tag{10}$$

and the coefficients

$$(a_j, c_j, e_j) \;=\; \begin{cases} \big(-\zeta\bar{z},\;\; \zeta\bar{z},\;\; 1-\zeta\big)\,, & j = 0\,, \\ \big(-\zeta\bar{z},\;\; \bar{z}^2,\;\; (1-\zeta)(1-\bar{z})\big)\,, & j = 1\,, \\ \big(-\zeta\bar{z}^2,\;\; \zeta\bar{z}^2,\;\; 1-\zeta\big)\,, & j = 2\,. \end{cases} \tag{11}$$

Note that these quadratics are related to the original z and $\bar{z}$ variable via $1 - z = D_0/D$, $1 - z - \bar{z} = D_1/D$ and $1 - z\bar{z} = D_2/D$. The discriminant of D_0 is the perfect square so D_0 can be factorized into $D_0 = \big(1 - \bar{z}x\big)\big(\zeta x + 1 - \zeta\big)$. The discriminants of D_1 and D_2 are not squares and they are the source of the elliptic sector.

With these notations, the $F_R(\zeta)$ integral can be rewritten as

$$F_R(\zeta) = \int_0^1 d\bar{z} \int_0^1 dx\, \big[\,\mathrm{ker}_1\, P_1 + \mathrm{ker}_2\, P_2\big]\,, \tag{12}$$

where the kernels $\mathrm{ker}_{1,2}$ are rational functions of x and $\bar{z}$,

$$\mathrm{ker}_1 = -\frac{\zeta(1-\zeta)\,\bar{z}^2\; x(x-1)}{D\, D_1}\,, \qquad \mathrm{ker}_2 = -\frac{\zeta^2(1-\zeta)\,\bar{z}^3\; x^2(x-1)^2}{D_0^2\, D_2}\,. \tag{13}$$

We then perform the partial fractioning in x for each channel, which separates the pole that carries the square root from the poles that do not. Explicitly we have $\mathrm{ker}_{1,2} = K_{1,2} + \mathrm{red}_{1,2}$ and

$$\begin{aligned} K_1 &= \frac{(\zeta-1)\,\bar{z}(1-\bar{z})}{D_1}, \quad \mathrm{red}_1 = -\frac{\bar{z}\, x_D}{x - x_D}\,, \\ K_2 &= \frac{(\zeta-1)\,\bar{z}}{(1-\bar{z})^2\, D_2}\,, \quad \mathrm{red}_2 = \frac{\bar{z}\,(\zeta-1)\,\big[\,\zeta\bar{z}(2-\bar{z})\, x^2 + \big(\zeta\bar{z}^2 - 2\zeta\bar{z} + \bar{z} - \zeta\big)\, x + \zeta - 1\,\big]}{(1-\bar{z})^2\,\big(1 - \bar{z}x\big)^2\big(\zeta x + 1 - \zeta\big)^2}\,. \end{aligned} \tag{14}$$

Here K_1 and K_2 are irreducible kernels and they are already introduced in Ref. [1] with an additional factor $\bar{z}$ due to a change of variable from t to x. The remainders red_1 and red_2 are rational in x with rational letters, so they will only give rise to polylogarithms.

Although the partial fractioning is exact, it does not make both channels separately integrable, and the difference between them dictates how the result must be organized. The obstruction sits at the corner of the integration region. As the outer variable approaches $\bar{z} = 1$, the root $x = 1/\bar{z}$ of D_0 moves onto the endpoint $x = 1$ of the inner integration, and there the two remaining quadratics vanish to different orders,

$$D_1\big|_{x=1/\bar{z}} = -\zeta\,(1-\bar{z})\,, \qquad D_2\big|_{x=1/\bar{z}} = \zeta\,(1-\bar{z})^2/\bar{z}\,, \tag{15}$$

a simple pole and a double pole. In the first channel K_1 carries the factor $\bar{z}(1-\bar{z})$, which vanishes as $\bar{z} \to 1$, and red_1 has its pole at x_D, away from the endpoint. So both pieces are integrable over $\bar{z}$ on their own. In the second channel K_2 carries $\bar{z}/(1-\bar{z})^2$ and red_2 carries the same $(1-\bar{z})^{-2}$ in its denominator, so each diverges like $(1-\bar{z})^{-2}\log^2(1-\bar{z})$ as the endpoint is approached. The divergence will cancel when summing the two pieces, but neither piece is integrable by itself. There are two possible ways to resolve this problem. We can introduce a regulator for $\bar{z} \to 1$ limit and then take the regulator to zero after integration. Alternatively, we can introduce a subtraction term that cancels the divergence in red_2 and add it to K_2. However, either approach will make the calculation more complicated. Thus, we will keep the ker_2 as a whole kernel and write

$$F_R(\zeta) = F_{\mathrm{red}_1}(\zeta) + F_{K_1}(\zeta) + F_{R_2}(\zeta)\,, \tag{16}$$

with three finite pieces defined as

$$\begin{aligned} F_{\mathrm{red}_1}(\zeta) &= \int_0^1 d\bar{z} \int_0^1 dx\ \mathrm{red}_1\, P_1(z,\bar{z})\,, \qquad F_{K_1}(\zeta) = \int_0^1 d\bar{z} \int_0^1 dx\ K_1\, P_1(z,\bar{z})\,, \\ F_{R_2}(\zeta) &= \int_0^1 d\bar{z} \int_0^1 dx\ \big[\mathrm{red}_2 + K_2\big]\, P_2(z,\bar{z})\,. \end{aligned} \tag{17}$$

The decomposition follows from the Galois symmetry. F_{K_1} and F_{R_2} contain one square root, of the discriminant of D_1 and of D_2 respectively and F_{red_1} contains neither. Flipping the sign of either square root leaves the decomposition unchanged and leaves the integral $F_R(\zeta)$ invariant, as it must be for a single-valued function on the physical region. In the next section, we will show that the two square roots in F_{K_1} and F_{R_2} are not independent, and the difference

$$\Delta(\zeta) \;\equiv\; F_{R_2}(\zeta) - F_{K_1}(\zeta) \tag{18}$$

is polylogarithmic. Eventually this will allow us to write the final result as

$$F_R(\zeta) \;=\; 2\,F_{K_1}(\zeta) \;+\; P(\zeta)\,, \qquad P(\zeta) \;\equiv\; F_{\mathrm{red}_1}(\zeta) + \Delta(\zeta)\,, \tag{19}$$

and our goal in this paper is to obtain the closed analytic form for both elliptic piece $F_{K_1}(\zeta)$ and polylogarithmic piece $P(\zeta)$.

III. THE ELLIPTIC CURVE AND THE SUNRISE

In this section, we will study the two elliptic curves described by the two irreducible kernels K_1 and K_2. In particular, we will show that they are the same curve and that it is the same curve as the sunrise integral. Then we will be able to further extract the polylogarithmic contribution from $F_{R_2}(\zeta)$.

A. Elliptic curve in EEC

After the partial fraction decomposition in the inner variable x, the two irreducible kernels carry the square roots of the discriminants of D_1 and D_2 in that variable. These discriminants are the quartic polynomials

$$\begin{aligned} Q_1(\bar{z}) &= \left(\bar{z}^2 - \bar{z} + 2\zeta^2 - \zeta\right)^2 + 4\zeta^3(1-\zeta) \\ &= \bar{z}^4 - 2\bar{z}^3 + (1 - 2\zeta + 4\zeta^2)\,\bar{z}^2 + 2\zeta(1-2\zeta)\,\bar{z} + \zeta^2\,, \\ Q_2(\bar{z}) &= \zeta^2\bar{z}^4 - 2\zeta\,\bar{z}^3 + (1 + 4\zeta - 2\zeta^2)\,\bar{z}^2 - 2\zeta\,\bar{z} + \zeta^2\,. \end{aligned} \tag{20}$$

Both quartics are positive for $0 < \zeta < 1$ along the real $\bar{z}$ axis. For Q_1 this follows directly from the first line of Eq. (20), a square plus a positive number. For Q_2, one has $Q_2(0) = \zeta^2 > 0$, while for $\bar{z} \neq 0$ the variable $v = \bar{z} + 1/\bar{z}$ gives the palindromic form $Q_2/\bar{z}^2 = (\zeta v - 1)^2 + 4\zeta(1-\zeta)$. The outer integration therefore never approaches a branch point in the physical region, and the integrands of Eq. (17) are real on the whole domain, with all their singularities on the boundary of the unit square. Moreover, the two quartics have the same discriminant, $\mathrm{disc}_{\bar{z}}\, Q_1 = \mathrm{disc}_{\bar{z}}\, Q_2 = 256\,\zeta^6(1-\zeta)^2(1+8\zeta)$, and hence the same singular fibers at $\zeta \in \{0, 1, -1/8, \infty\}$.

It turns out that the two quartics are related by a Möbius transformation $w = \bar{z}/(\bar{z}-1)$, which is an involution of the $\bar{z}$ line that fixes $\bar{z} = 0$ and sends the endpoint $\bar{z} = 1$ to $w = \infty$. Explicitly we find

$$Q_2(\bar{z}) = (\bar{z}-1)^4\, Q_1(w)\,, \qquad \frac{d\bar{z}}{\sqrt{Q_2(\bar{z})}} = -\frac{dw}{\sqrt{Q_1(w)}}\,. \tag{21}$$

Then the measure in F_{R_2}, $\bar{z}\,d\bar{z}/[(1-\bar{z})^2\sqrt{Q_2(\bar{z})}]$, becomes $w(1-w)\,dw/\sqrt{Q_1(w)}$ in the variable w, which is the same as the measure of F_{K_1}. This means both F_{R_2} and F_{K_1} are integrals over the same elliptic curve $\mathcal{C}_\zeta : y^2 = Q_1(\bar{z})$, with the same weight, but over different contours. The interval $\bar{z} \in [0, 1]$ maps to $w \in (-\infty, 0]$. The equivalence of the two curves is also manifest from

their j-invariants, which agree identically in ζ,

$$j(\zeta) \;=\; \frac{(1+2\zeta)^3\big(8\zeta^3-12\zeta^2+6\zeta+1\big)^3}{\zeta^6\,(1-\zeta)^2\,(1+8\zeta)}\,. \tag{22}$$

As observed in Ref. [1], the equal-mass two-loop sunrise integral is also described by the same elliptic curve $\mathcal{C}_\zeta$. Here we make the identification more precise. The sunrise is the first Feynman integral known to require elliptic functions for its evaluation, and it has been studied extensively in the literature. Explicitly, the sunrise integral in $d=2$ dimensions is defined as [31–33]

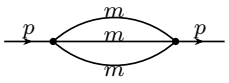

$$\;=\; \int\frac{d^2\ell_1\,d^2\ell_2}{\pi^2}\,\frac{1}{(\ell_1^2-m^2)\,(\ell_2^2-m^2)\,\big((p-\ell_1-\ell_2)^2-m^2\big)}\,, \tag{23}$$

and we write $p^2=S$ and $m^2\to m^2-i0$ for the $i\epsilon$ prescription. In $d=2$ dimension, the integral is finite and depends only on the ratio S/m^2. With the $\mathcal{U}\mathcal{F}$ polynomials $\mathcal{U}=x_1x_2+x_2x_3+x_3x_1$ and $\mathcal{F}=m^2\,(x_1{+}x_2{+}x_3)\,\mathcal{U}-S\,x_1x_2x_3$, the Feynman-parametric representation of the sunrise integral takes the form

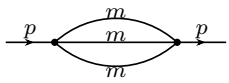

$$\;=\; \int_0^\infty d^3x\;\;\frac{\delta\big(1-x_1-x_2-x_3\big)}{\mathcal{F}}\,. \tag{24}$$

The sunrise curve is read off from $\mathcal{F}$ by itself. With the Cheng-Wu theorem [67], we can set $x_3=1$. We can also set $m=1$ for convenience and recover the mass dependence by dimensional analysis in the end. Then we find that $\mathcal{F}$ is a quadratic in x_1,

$$\mathcal{F}\big|_{x_3=1,\,m=1} = (x_2{+}1)\,x_1^2+\big(x_2^2+(3-S)\,x_2+1\big)\,x_1+x_2\,(x_2{+}1)\,, \tag{25}$$

and completing the square in x_1 brings in the square root of its discriminant,

$$\begin{aligned}\mathrm{disc}_{x_1}\mathcal{F} &= \big(x_2^2+(3-S)\,x_2+1\big)^2-4\,x_2\,(x_2{+}1)^2 \;=\; Q_{\rm sun}(x_2;S)\,,\\ \Rightarrow Q_{\rm sun}(u;S) &= u^4-2(S-1)\,u^3+(S^2-6S+3)\,u^2-2(S-1)\,u+1\,.\end{aligned} \tag{26}$$

The sunrise curve is the double cover $y^2=Q_{\rm sun}(u;S)$ of the u-line branched over the four roots of this quartic. Its j-invariant is

$$j_{\rm sun}(S) = \frac{(S-3)^3\big(S^3-9S^2+3S-3\big)^3}{S^2\,(S-1)^3\,(S-9)}\,, \tag{27}$$

whose poles sit at the four singular fibers of the family, $S/m^2=0,1,9,\infty$: the normal threshold $S=9m^2$, the pseudo-threshold $S=m^2$, and the two ends. They are exactly the zeros of $\mathrm{disc}_u\,Q_{\rm sun}=256\,S^2(S-1)^3(S-9)$.

To compare the sunrise curve with the EEC curve, we go back to the projective coordinate and choose the following parameterization of the Feynman parameters and kinematic variable S,

$$(x_1 : x_2 : x_3) = \big(\bar{z} \,:\, \bar{z}x - 1 \,:\, 1 - \bar{z}\big)\,, \qquad S = m^2\,\frac{\zeta - 1}{\zeta}\,, \tag{28}$$

under which one finds the exact identity

$$\bar{z}\,D_1(x) \;=\; -\frac{\zeta}{m^2}\,\mathcal{F}(x_1, x_2, x_3)\,. \tag{29}$$

The prefactor $\bar{z}$ on the left of Eq. (29) is invisible to the geometry, since $\mathrm{disc}_x(\bar{z}D_1) = \bar{z}^2 Q_1$ differs from Q_1 by a square. At the level of the quartics themselves the same identification reads

$$Q_1(\bar{z}) = \zeta^2(1-\bar{z})^4\,Q_{\rm sun}\Big(\frac{\bar{z}}{1-\bar{z}}; S\Big)\,, \qquad Q_2(\bar{z}) = \zeta^2\,Q_{\rm sun}(-\bar{z}; S)\,, \tag{30}$$

In both relations the prefactor is ζ^2 times a perfect square, so both double covers are isomorphic to the sunrise curve: the second channel reaches it by the sign flip $u = -\bar{z}$ alone and needs no Möbius map, while the first needs $u = \bar{z}/(1-\bar{z})$, and the two substitutions differ by the involution of Eq. (21). Substituting $S = (\zeta-1)/\zeta$ into Eq. (27) returns Eq. (22) identically in ζ, and the singular fibers line up one to one: $S/m^2 = \infty, 0, 9, 1$ correspond to $\zeta = 0, 1, -1/8, \infty$. In particular the fourth singular point $\zeta = -1/8$ of the family, which looks accidental in the EEC variable, is the normal threshold $S = 9m^2$ of the sunrise. Under Eq. (28), the physical region $0 < \zeta < 1$ is mapped to $S/m^2 = (\zeta-1)/\zeta < 0$, namely the Euclidean region of the sunrise integral, below every threshold. This is why the EEC integral is real throughout and why nothing singular happens between the endpoints. The collinear and back-to-back limits correspond to $S/m^2 \to -\infty$ and $S/m^2 \to 0$, respectively.

The periods of $\mathcal{C}_\zeta$ are annihilated by the sunrise Picard-Fuchs operator [31–33, 68]

$$L_{\rm PF} \;=\; \zeta(\zeta-1)(8\zeta+1)\,\partial^2 \;+\; (24\zeta^2 - 14\zeta - 1)\,\partial \;+\; 2(4\zeta - 1)\,, \tag{31}$$

with ∂ the derivative with respect to ζ. Its four regular singular points $\zeta = 0, 1, -1/8, \infty$ are maximally unipotent: they are the four cusps of $\Gamma_1(6)$, the modular group of the equal-mass sunrise family [32, 33, 61]. The same operator annihilates the periods of both $y^2 = Q_1$ and $y^2 = Q_2$. Explicitly, we have

$$L_{\rm PF}\big[Q_j^{-1/2}\big] = \frac{d}{d\bar{z}}\Big[U_j\,Q_j^{-3/2}\Big]\,, \qquad j = 1, 2\,, \tag{32}$$

with the factors

$$U_1 = -\bar{z}(\bar{z}-1)(2\bar{z}-1)\big[(4\zeta-1)\,\bar{z}(\bar{z}-1) + \zeta(2\zeta+1)\big]\,,$$

$$U_2 = \bar{z}(\bar{z}-1)(\bar{z}+1)\big[\zeta(2\zeta+1)\bar{z}^2 - (4\zeta^2-2\zeta+1)\bar{z} + \zeta(2\zeta+1)\big]\,. \tag{33}$$

Since $U_j(0) = U_j(1) = 0$ identically in ζ, the total derivative in Eq. (32) gives no boundary contribution on the physical contour. This also confirms that the two elliptic curves in NNLO EEC as well as the sunrise curve are identical.

B. Further decomposition of F_{R_2}

The equivalence of the two curves does not guarantee that the two integrals $F_{K_1}(\zeta)$ and $F_{R_2}(\zeta)$ will give the same elliptic functions, given both the contours and the transcendental integrands are different. In this subsection, we will show that the difference $\Delta(\zeta) = F_{R_2}(\zeta) - F_{K_1}(\zeta)$ is polylogarithmic, and we will give it in closed form.

To study the transcendentality of $\Delta(\zeta)$, we need to derive the differential equations satisfied by $F_{K_1}(\zeta)$ and $F_{R_2}(\zeta)$. It turns out that $F_{K_1}(\zeta)$ does not satisfy a second-order differential equation by itself. Differentiating it twice in ζ produces one further two-fold integral, which takes the following form

$$S_0(\zeta) \;=\; \int_0^1 d\bar{z} \int_0^1 dx\, \frac{P_1(z,\bar{z})}{D_1(x)}\,, \tag{34}$$

with D_1 the quadratic of Eq. (11), $z = \zeta\bar{z}\,x(x-1)/D$, and P_1 as in Eq. (6). Since $K_1 = (\zeta-1)\bar{z}(1-\bar{z})/D_1$, F_{K_1} and S_0 differ only by the rational factor $(\zeta-1)\bar{z}(1-\bar{z})$ in the integrand. Since $D_1 > 0$ on the unit square except at the two corners $(x,\bar{z}) = (0,1)$ and $(1,1)$, where it vanishes linearly $(D_1|_{\bar{z}=1} = \zeta\,x(1-x))$, S_0 is also finite. F_{K_1} and S_0 then satisfy an inhomogeneous second-order system with rational coefficients,

$$\begin{aligned} \mathcal{L}\big[F_{K_1}\big] \;&=\; E(\zeta) \;+\; \alpha\, S_0 \;+\; \beta\, F_{K_1}\,, \\ \mathcal{L}\big[S_0\big] \;&=\; E'(\zeta) \;+\; \alpha'\, S_0 \;+\; \beta'\, F_{K_1}\,, \end{aligned} \tag{35}$$

in which the operator $\mathcal{L}$ is,

$$\mathcal{L} \;=\; \zeta(\zeta-1)(8\zeta+1)\,\partial^2 \;+\; (8\zeta^2+1)\,\partial \;-\; \frac{2\zeta+1}{\zeta}\,, \tag{36}$$

and

$$\alpha = 1+\zeta-8\zeta^2\,, \quad \beta = \frac{32\zeta^3-18\zeta^2+1}{\zeta(\zeta-1)}\,, \quad \alpha' = \frac{8\zeta^2-10\zeta-1}{\zeta}\,, \quad \beta' = \frac{6}{\zeta(1-\zeta)}\,. \tag{37}$$

$\mathcal{L}$ is connected to the Picard-Fuchs operator in Eq. (31) by $\mathcal{L} = \zeta \circ L_{\rm PF} \circ \zeta^{-1}$. The fact that $\mathcal{L}$ contains derivatives of at most second order and that the two equations are coupled to only rational

functions indicates that the result is at most elliptic. No geometry beyond the elliptic curve, such as a K3 or Calabi–Yau period, can appear in the final result.

The second integral in $F_R(\zeta)$ is treated in the same way, with a source and a companion of its own. The companion is again a double integral of the type of Eq. (34), with P_2/D_2 in place of P_1/D_1, so that

$$\mathcal{L}\big[F_{R_2}\big] \;=\; E_{R_2} \;-\; \alpha \int_0^1 d\bar{z} \int_0^1 dx\, \frac{P_2(z,\bar{z})}{D_2(x)} \;+\; \beta\, F_{R_2}\,, \tag{38}$$

with the same coefficients α, β as in Eq. (35). Both sources E and E_{R_2} are harmonic polylogarithms of ζ over the alphabet $\{0,1\}$ with rational coefficients in ζ: E is of weight at most four, and E_{R_2}, which carries a ζ_5 and a $\pi^2\zeta_3$ channel that E does not, of weight at most five. They are given in Eqs. (B1) and (B4) of App. B.

It turns out the additional integrals that show up on the RHS after differentiation are the same as in F_{K_1}, namely

$$\int_0^1 d\bar{z} \int_0^1 dx\, \frac{P_2(z,\bar{z})}{D_2(x)} \;=\; -\,S_0(\zeta)\,. \tag{39}$$

Then we have the entire differential system for all integrals,

$$\begin{aligned}
\mathcal{L}\big[F_{K_1}\big] \;&=\; E \;+\; \alpha\, S_0 \;+\; \beta\, F_{K_1}\,,\\
\mathcal{L}\big[F_{R_2}\big] \;&=\; E_{R_2} \;+\; \alpha\, S_0 \;+\; \beta\, F_{R_2}\,,\\
\mathcal{L}\big[S_0\big] \;&=\; E' \;+\; \alpha' S_0 \;+\; \beta' F_{K_1}\,,\\
\mathcal{L}\big[S_0\big] \;&=\; E'_{R_2} \;+\; \alpha' S_0 \;+\; \beta' F_{R_2}\,.
\end{aligned} \tag{40}$$

In particular, the difference of the last two equations give,

$$\beta'\Delta = E' - E'_{R_2} \quad\Rightarrow\quad \Delta \;=\; \frac{\zeta(1-\zeta)}{6}\left(E' - E'_{R_2}\right). \tag{41}$$

Since both E' and E'_{R_2}, given in Eqs. (B2) and (B5) of App. B, are polylogarithmic, Δ is also polylogarithmic. Therefore, we arrive at the final form

$$F_R(\zeta) \;=\; 2\,F_{K_1}(\zeta) \;+\; P(\zeta) \;=\; 2\,F_{K_1}(\zeta) \;+\; F_{\mathrm{red}_1}(\zeta) + \Delta(\zeta)\,. \tag{42}$$

We will discuss their analytic forms in the following sections.

IV. ANALYTIC RESULTS

In this section, we provide the analytic expression of EEC at NNLO. As discussed in the previous section, the remaining integral is further written as a single elliptic piece $F_{K_1}(\zeta)$ and a

sum of polylogarithmic pieces $P(\zeta)$. We calculate the exact form of $P(\zeta)$ and combine it with the existing HPL contribution in Ref. [1]. For the elliptic sector, we derive the differential operator and solve the system analytically. The result is then expressed in terms of iterated Eisenstein integrals.

A. The polylogarithmic sector

For the polylogarithmic sector, $P(\zeta) = F_{\text{red}_1}(\zeta) + \Delta(\zeta)$, we can directly perform the two integrations using HyperInt [69] in Maple, and the result can be expressed in terms of HPLs up to weight 5. Explicitly we find the following analytic form,

$$
\begin{aligned}
P(\zeta) =& \Big[4(\zeta-1) + \frac{6\zeta^3-4\zeta^2-5\zeta+4}{6(\zeta-1)}\pi^2 + \frac{(2\zeta-3)\left(3\zeta^2-11\zeta+7\right)}{2(\zeta-1)}\zeta_3 \\
&\quad - \frac{\zeta}{15(\zeta-1)}\pi^4 - \frac{\zeta\left(\zeta^2-2\zeta+3\right)}{24(\zeta-1)}\pi^2\zeta_3 - \frac{\zeta\left(14\zeta^2-28\zeta-19\right)}{4(\zeta-1)}\zeta_5 \Big] \\
&+ \Big[\frac{(\zeta-2)(2\zeta-1)}{6(\zeta-1)}\pi^2 + \frac{6\zeta^3-14\zeta^2+11\zeta-2}{\zeta-1}\zeta_3 + \frac{\zeta\left(\zeta^2-2\zeta-1\right)}{60(\zeta-1)}\pi^4 \Big] H_0(\zeta) \\
&+ \Big[-4(\zeta-1) - \frac{13\zeta^2-21\zeta+7}{12(\zeta-1)}\pi^2 + \frac{\zeta\left(12\zeta^2-25\zeta+15\right)}{2(\zeta-1)}\zeta_3 \\
&\quad + \frac{\zeta\left(4\zeta^2-8\zeta-11\right)}{240(\zeta-1)}\pi^4 \Big] H_1(\zeta) \\
&+ \Big[\left(2\zeta^2-2\zeta+1\right) - \frac{(\zeta-1)(3\zeta-1)}{12}\pi^2 - \frac{\zeta\left(\zeta^2-2\zeta-1\right)}{4(\zeta-1)}\zeta_3 \Big] H_{0,0}(\zeta) \\
&+ \Big[\frac{2\zeta^3-10\zeta^2+9\zeta-2}{\zeta-1} + \frac{6\zeta^3-14\zeta^2+7\zeta-2}{6(\zeta-1)}\pi^2 + \frac{\zeta\left(\zeta^2-2\zeta+5\right)}{4(\zeta-1)}\zeta_3 \Big] H_2(\zeta) \\
&+ \Big[(\zeta-2)(2\zeta-1) - \frac{3\zeta^3-6\zeta^2+3\zeta-2}{12(\zeta-1)}\pi^2 - \frac{\zeta\left(\zeta^2-2\zeta-5\right)}{4(\zeta-1)}\zeta_3 \Big] H_{1,0}(\zeta) \\
&+ \Big[(\zeta-1)(2\zeta-3) + \frac{12\zeta^3-27\zeta^2+13\zeta-2}{12(\zeta-1)}\pi^2 + \frac{\zeta\left(\zeta^2-2\zeta+3\right)}{4(\zeta-1)}\zeta_3 \Big] H_{1,1}(\zeta) \\
&+ \Big[\frac{6\zeta^3-8\zeta^2+2\zeta+1}{2(\zeta-1)} - \frac{\zeta\left(\zeta^2-2\zeta+7\right)}{24(\zeta-1)}\pi^2 \Big] H_3(\zeta) \\
&+ \Big[-\frac{5\zeta^2-9\zeta+2}{2(\zeta-1)} + \frac{\zeta}{4(\zeta-1)}\pi^2 \Big] H_{2,0}(\zeta) + \Big[\frac{\zeta}{2} - \frac{\zeta}{12(\zeta-1)}\pi^2 \Big] H_{1,0,0}(\zeta) \\
&+ \Big[\frac{6\zeta^2-11\zeta+6}{2} - \frac{\zeta\left(\zeta^2-2\zeta+3\right)}{24(\zeta-1)}\pi^2 \Big] H_{2,1}(\zeta) + \frac{\zeta}{6(\zeta-1)}\pi^2 H_{1,1,0}(\zeta) \\
&+ \Big[\frac{6\zeta^3-7\zeta^2-\zeta+1}{2(\zeta-1)} - \frac{\zeta\left(\zeta^2-2\zeta+13\right)}{24(\zeta-1)}\pi^2 \Big] H_{1,2}(\zeta) \\
&+ \Big[(\zeta-1)(3\zeta-4) - \frac{\zeta\left(\zeta^2-2\zeta+7\right)}{24(\zeta-1)}\pi^2 \Big] H_{1,1,1}(\zeta) \\
&- \frac{\zeta\left(5\zeta^2-11\zeta+4\right)}{2(\zeta-1)} H_4(\zeta) + \frac{3\zeta^3-7\zeta^2+2\zeta-1}{\zeta-1} H_{3,0}(\zeta) + \frac{5\zeta^2-7\zeta+4}{2} H_{3,1}(\zeta)
\end{aligned}
$$

$$
\begin{aligned}
&- \frac{\zeta^2-2\zeta+2}{2}\, H_{2,0,0}(\zeta) - \frac{2\left(2\zeta^3-4\zeta^2-\zeta+1\right)}{\zeta-1}\, H_{2,2}(\zeta) + \frac{\zeta\,(\zeta-1)}{2}\, H_{2,1,0}(\zeta) \\
&+ \left(3\zeta^2-5\zeta+4\right)\, H_{2,1,1}(\zeta) - \frac{5\zeta^3-8\zeta^2+1}{2\,(\zeta-1)}\, H_{1,3}(\zeta) + \frac{6\zeta^3-15\zeta^2+9\zeta-2}{2\,(\zeta-1)}\, H_{1,2,0}(\zeta) \\
&+ \frac{5\zeta^2-11\zeta+5}{2}\, H_{1,2,1}(\zeta) - \frac{(\zeta-1)^2}{2}\, H_{1,1,0,0}(\zeta) - \frac{8\zeta^3-15\zeta^2+\zeta+2}{2\,(\zeta-1)}\, H_{1,1,2}(\zeta) \\
&+ \frac{(\zeta-1)^2}{2}\, H_{1,1,1,0}(\zeta) + 3\,(\zeta-1)^2\, H_{1,1,1,1}(\zeta) + \frac{\zeta\,(\zeta-1)}{2}\, H_5(\zeta) \\
&+ \frac{3\zeta\left(\zeta^2-2\zeta-1\right)}{4\,(\zeta-1)}\, H_{4,0}(\zeta) + \frac{\zeta\left(5\zeta^2-10\zeta+1\right)}{4\,(\zeta-1)}\, H_{4,1}(\zeta) - \frac{\zeta\left(\zeta^2-2\zeta-1\right)}{4\,(\zeta-1)}\, H_{3,0,0}(\zeta) \\
&+ \frac{3\zeta\,(\zeta-1)}{4}\, H_{3,2}(\zeta) + \frac{\zeta\,(\zeta-1)}{2}\, H_{3,1,0}(\zeta) + \frac{\zeta\left(3\zeta^2-6\zeta-1\right)}{2\,(\zeta-1)}\, H_{3,1,1}(\zeta) \\
&+ \frac{\zeta\left(\zeta^2-2\zeta+2\right)}{\zeta-1}\, H_{2,3}(\zeta) + \frac{3\zeta\,(\zeta-1)}{4}\, H_{2,2,0}(\zeta) + \frac{\zeta\left(7\zeta^2-14\zeta+9\right)}{4\,(\zeta-1)}\, H_{2,2,1}(\zeta) \\
&- \frac{\zeta\,(\zeta-1)}{4}\, H_{2,1,0,0}(\zeta) + \frac{\zeta\left(5\zeta^2-10\zeta+7\right)}{4\,(\zeta-1)}\, H_{2,1,2}(\zeta) + \frac{\zeta\,(\zeta-1)}{2}\, H_{2,1,1,0}(\zeta) \\
&+ 2\zeta\,(\zeta-1)\, H_{2,1,1,1}(\zeta) + \frac{\zeta\left(\zeta^2-2\zeta+5\right)}{2\,(\zeta-1)}\, H_{1,4}(\zeta) + \frac{\zeta\left(3\zeta^2-6\zeta-7\right)}{4\,(\zeta-1)}\, H_{1,3,0}(\zeta) \\
&+ \frac{\zeta\left(5\zeta^2-10\zeta+9\right)}{4\,(\zeta-1)}\, H_{1,3,1}(\zeta) - \frac{\zeta\left(\zeta^2-2\zeta-1\right)}{4\,(\zeta-1)}\, H_{1,2,0,0}(\zeta) \\
&+ \frac{3\zeta\left(\zeta^2-2\zeta+5\right)}{4\,(\zeta-1)}\, H_{1,2,2}(\zeta) + \frac{\zeta\,(\zeta-1)}{2}\, H_{1,2,1,0}(\zeta) + \frac{3\zeta\,(\zeta-1)}{2}\, H_{1,2,1,1}(\zeta) \\
&+ \frac{\zeta\left(2\zeta^2-4\zeta+3\right)}{2\,(\zeta-1)}\, H_{1,1,3}(\zeta) + \frac{\zeta\left(3\zeta^2-6\zeta-1\right)}{4\,(\zeta-1)}\, H_{1,1,2,0}(\zeta) + \frac{7\zeta\,(\zeta-1)}{4}\, H_{1,1,2,1}(\zeta) \\
&- \frac{\zeta\,(\zeta-1)}{4}\, H_{1,1,1,0,0}(\zeta) + \frac{\zeta\left(5\zeta^2-10\zeta+11\right)}{4\,(\zeta-1)}\, H_{1,1,1,2}(\zeta) + \frac{\zeta\,(\zeta-1)}{2}\, H_{1,1,1,1,0}(\zeta) \\
&+ 2\zeta\,(\zeta-1)\, H_{1,1,1,1,1}(\zeta)\,. \qquad (43)
\end{aligned}
$$

The alphabet for $P(\zeta)$ is $\{\zeta, 1-\zeta\}$, and unlike the NLO result in Ref. [6] or the HPL part in Ref. [1], there is no square-root letter, $(1-\sqrt{\zeta})/(1+\sqrt{\zeta})$ appearing in the arguments. The transcendental weight is at most five and is not uniform. We verify the analytic expression against the numerical integration with randomly ζ values.

B. The elliptic sector

1. *Solving the system*

With the further decomposition described in Sec. III, the only remaining integral to compute is $F_{K_1}(\zeta)$. Recall that we have the following equations from Eq. (40),

$$
\mathcal{L}[F_{K_1}] = E + \alpha S_0 + \beta F_{K_1}\,, \qquad \mathcal{L}[S_0] = E' + \alpha' S_0 + \beta' F_{K_1}\,, \qquad (44)
$$

where E and E' are both harmonic polylogarithmic, given explicitly in Eqs. (B1) and (B2) of App. B. To solve the system, we can write it as the sum of the solution to Picard-Fuchs operator and the residual terms. First of all, we write the following ansatz

$$F_{K_1} = c_1 S_0 + c_2 S_0^{'} + \Psi, \quad \text{with} \quad S_0^{'} \equiv \partial S_0\,, \tag{45}$$

and $c_{1,2}$ rational. Substituting into the second equation in Eq. (44), we find

$$\big(\mathcal{L} - \alpha' - \beta' c_1 - \beta' c_2\,\partial\big) S_0 = E' + \beta'\Psi\,. \tag{46}$$

Demanding $\mathcal{L} - \alpha' - \beta' c_1 - \beta' c_2\,\partial = L_{\rm PF}$ gives $c_1 = \frac{1}{3}\,\zeta(\zeta-1)(8\zeta-5)$ and $c_2 = \frac{1}{3}\,\zeta(8\zeta+1)(\zeta-1)^2$. Then the second equation of Eq. (44) becomes $L_{\rm PF} S_0 = E' + \beta'\Psi$. We also substitute the ansatz into the first equation,

$$\begin{aligned}\left[\partial^2 - \frac{8\zeta^2-14\zeta-3}{\zeta(\zeta-1)(8\zeta+1)}\,\partial - \frac{64\zeta^3-42\zeta^2-3\zeta-4}{\zeta^2(\zeta-1)^2(8\zeta+1)}\right]\Psi \\ = \frac{E}{\zeta(\zeta-1)(8\zeta+1)} - \frac{32\zeta^2-3\zeta+1}{3\,\zeta(8\zeta+1)}\,E' - \frac{\zeta-1}{3}\,\partial E'\end{aligned} \tag{47}$$

The solution Ψ to this equation is purely polylogarithmic. We write an ansatz of HPLs of ζ over $\{0,1\}$ with rational function coefficients and solve it by series expansion in $\zeta \to 0$ limit. The final expression reads

$$\begin{aligned}\Psi(\zeta) = \frac{1}{4}\Big[&-8\,(\zeta-1) + 8\,(\zeta-1)\;H_1(\zeta) + 2\,(\zeta-1)\;H_{0,0}(\zeta) - 4\,\big(2\zeta^2-4\zeta+1\big)\;H_{0,1}(\zeta) \\ &+ 2\,(\zeta-1)\;H_{1,0}(\zeta) - 8\,(\zeta-1)^2\;H_{1,1}(\zeta) - \big(12\zeta^2-8\zeta-1\big)\;H_{0,0,1}(\zeta) \\ &+ 2\,(\zeta-1)\;H_{0,1,0}(\zeta) - 6\,(\zeta-1)\,(2\zeta-1)\;H_{0,1,1}(\zeta) - 2\,(\zeta-1)\;H_{1,0,0}(\zeta) \\ &- \big(12\zeta^2-14\zeta+5\big)\;H_{1,0,1}(\zeta) - 12\,(\zeta-1)^2\;H_{1,1,1}(\zeta)\Big] - \frac{3\zeta_3}{4}\,\big(4\zeta^2-10\zeta+7\big) \\ &+ \frac{\pi^2}{24}\Big[-4\,\big(2\zeta^2+\zeta-2\big) - 4\,(\zeta-1)\;H_0(\zeta) + (10\zeta-7)\;H_1(\zeta)\Big] \\ &+ (\zeta-1)\left(\zeta-\frac{1}{4}\right)\Bigg\{\frac{2}{3}\Big[2\,H_{0,0,0,1}(\zeta) - H_{0,0,1,1}(\zeta) + H_{0,1,0,1}(\zeta) - 2\,H_{0,1,1,1}(\zeta) + 4H_{1,0,0,1}(\zeta) \\ &+ H_{1,0,1,1}(\zeta) + 3H_{1,1,0,1}(\zeta)\Big] + \frac{\pi^2}{6}\Big[H_{0,0}(\zeta) - 2H_{0,1}(\zeta) + H_{1,0}(\zeta) - 2\,H_{1,1}(\zeta)\Big] \\ &- \frac{2\zeta_3}{3}\Big[7\,H_0(\zeta) + 5\,H_1(\zeta)\Big] + \frac{2\pi^4}{45}\Bigg\}\,.\end{aligned} \tag{48}$$

The second equation, $L_{\rm PF} S_0 = E' + \beta'\Psi$, now has an explicit right-hand side. To solve this equation, we pass to the modular frame. Let ψ_1 and ψ_2 be the two solutions of $L_{\rm PF}$ at $\zeta = 0$, with ψ_1 holomorphic and normalized to $\psi_1(0) = 1$ and $\psi_2 = \psi_1 \log\zeta + \mathcal{O}(\zeta)$. Then we also define $\tilde{\tau}$ to be their ratio, $\tilde{\tau} = \frac{1}{2} + \frac{1}{2\pi i}\,\psi_2(\zeta)/\psi_1(\zeta)$, so that $2\pi i\,\big(\tilde{\tau} - \frac{1}{2}\big) = \log\zeta - 3\zeta + \frac{21}{2}\zeta^2 - \ldots$. The

collinear limit $\zeta \to 0$ is $\tilde{\tau} \to i\infty$. Since ζ is a Hauptmodul for $\Gamma_1(6)$ this map is invertible, and Eq. (51) below gives the inverse in closed form [32, 58]. The four singular points in the elliptic curve $\zeta = 0, 1, \infty, -\frac{1}{8}$ are then mapped to $\tilde{\tau} = i\infty, \frac{1}{2}, \frac{1}{3}, 0$. We further define

$$q = e^{2\pi i\left(\tilde{\tau}-\frac{1}{2}\right)}\,, \qquad L = \log q\,, \qquad \theta = q\,\frac{d}{dq} = \frac{1}{2\pi i}\frac{d}{d\tilde{\tau}}\,. \tag{49}$$

The physical region $0 < \zeta < 1$ is the line $\tilde{\tau} = \frac{1}{2} + is$, on which $q = e^{-2\pi s}$ is real and positive and s runs from ∞ in the collinear limit to 0 in the back-to-back limit. Thus we shift the power in q by $\frac{1}{2}$ in Eq. (49) which makes q, and with it every series below, real and positive on the physical line, at the price of alternating signs relative to the usual $\tilde{q} = e^{2\pi i\tilde{\tau}} = -q$.

The holomorphic solution to $L_{\rm PF}$, ψ_1, admits the following Taylor expansion in ζ with Franel numbers [70, 71],

$$\psi_1(\zeta) = \sum_{n\geq 0}(-1)^n\Big[\sum_{k=0}^{n}\binom{n}{k}^3\Big]\zeta^n = 1 - 2\zeta + 10\zeta^2 - 56\zeta^3 + 346\zeta^4 - \dots\,, \tag{50}$$

a modular form of weight one for $\Gamma_1(6)$ with a simple zero at the cusp $\zeta = \infty$ and no other zero. Everything in this frame can be built from the Dedekind eta function $\eta(\tilde{\tau}) = \tilde{q}^{1/24}\prod_{n\geq 1}(1-\tilde{q}^n)$. Writing $\eta_d \equiv \eta(d\tilde{\tau})$, the Hauptmodul (which is our angular variable), the period, and the two other factors that will be needed are eta quotients,

$$\begin{aligned}
&\zeta = -\frac{\eta_1^3\eta_6^9}{\eta_2^3\eta_3^9} = q + 3q^2 + 3q^3 - 5q^4 - 18q^5 + \dots\,, \qquad \psi_1 = \frac{\eta_2\eta_3^6}{\eta_1^2\eta_6^3} = 1 - 2q + 4q^2 - 2q^3 + \dots\,,\\
&1-\zeta = \frac{\eta_2^5\eta_6}{\eta_1\eta_3^5}\,, \qquad 1+8\zeta = \frac{\eta_1^8\eta_6^4}{\eta_2^4\eta_3^8}\,.
\end{aligned} \tag{51}$$

The frame and the operator are tied by the derivative rule

$$\theta\zeta = \psi_1^2\,\zeta(1-\zeta)(1+8\zeta)\,, \qquad \text{equivalently} \qquad \log\zeta = L + \log\frac{\zeta}{q} = L + 3q - \frac{3}{2}q^2 - 5q^3 + \dots\,, \tag{52}$$

The second form is the dictionary between the logarithm of the kinematic variable and the logarithm of q. It is also the reason why L carries transcendental weight one. The Wronskian of the Frobenius basis of $L_{\rm PF}$ at $\zeta = 0$ is $[\zeta(1-\zeta)(1+8\zeta)]^{-1}$, and the mirror map $q(\zeta)$ built from that basis inverts the first eta quotient of Eq. (51). We verify Eqs. (51), (50) and (52), together with $L_{\rm PF}\psi_1 = 0$ and the mirror-map statement, as exact rational q-series through q^{339}.

Recall that ψ_1 has a single simple zero, and that it sits exactly where ζ has its pole. The ring of modular forms of the group is therefore

$$M_k\left(\Gamma_1(6)\right) = \psi_1^k \cdot \mathrm{span}_{\mathbb{Q}}\{1, \zeta, \zeta^2, \dots, \zeta^k\}\,, \qquad \dim M_k\left(\Gamma_1(6)\right) = k+1\,, \tag{53}$$

which is the Riemann–Roch count for genus zero with four cusps. Odd weights occur because $-1 \notin \Gamma_1(6)$. The first cusp form appears only at $k = 4$, so weight-two and weight-three forms are all Eisenstein. We use Eq. (53) as an operational test rather than as a dimension count. A function is a modular form of modular weight k if and only if it is ψ_1^k times a polynomial in ζ of degree at most k. For NNLO EEC, we will need the following letters

$$\begin{aligned}
\omega_0 &\equiv \theta \log \zeta = \psi_1^2 \left(1 + 7\zeta - 8\zeta^2\right) , && \deg = 2 \le 2 , \quad \text{modular weight } 2 , \\
\omega_1 &\equiv -\theta \log(1-\zeta) = \psi_1^2 \left(\zeta + 8\zeta^2\right) , && \deg = 2 \le 2 , \quad \text{modular weight } 2 , \\
\psi_1 \omega_0 &= \psi_1^3 (1-\zeta)(1+8\zeta) , && \deg = 2 \le 3 , \quad \text{modular weight } 3 , \\
\zeta \psi_1 \omega_0 &= \psi_1 \theta \zeta = \psi_1^3 \zeta (1-\zeta)(1+8\zeta) , && \deg = 3 \le 3 , \quad \text{modular weight } 3 ,
\end{aligned} \tag{54}$$

where the first two letters are the HPL letters and the last two are new.

With these notations at hand, we can write for any g,

$$L_{\rm PF}\left(\psi_1\, g\right) = -\frac{\theta^2 g}{\zeta\, \psi_1 \omega_0} , \tag{55}$$

where we use $L_{\rm PF}\psi_1 = 0$ and Eq. (52). The denominator is the modular-weight-three letter of Eq. (54), and this is how the elliptic letter enters the answer. Applied to $g = S_0/\psi_1$ the identity turns this equation into

$$\theta^2 \left(\frac{S_0}{\psi_1}\right) = -\zeta\, \psi_1 \omega_0 \left(E' + \beta' \Psi\right) . \tag{56}$$

The second-order operator has become two antiderivatives, with the factor $\zeta\, \psi_1 \omega_0$ remaining in the integrand. That factor, like ω_0 and ω_1, is a power of ψ_1 times a polynomial in ζ, so the answer will be an iterated integral whose letters are modular forms. With Ψ of Eq. (48) the bracket on the right of Eq. (56) is an explicit polylogarithm.

2. *Iterated Eisenstein integrals*

To solve this equation, we need to introduce a set of iterated integrals in q [58]. Explicitly, we define the iterated Eisenstein integrals via

$$I(f_1, \ldots, f_n; q) = \theta^{-1}\left(f_1\, I(f_2, \ldots, f_n; q)\right) = \theta^{-1}\Big[f_1\, \theta^{-1}\left(f_2 \cdots \theta^{-1}(f_n)\right)\Big] , \tag{57}$$

with the convention $I(\,;q) = 1$. Here θ^{-1} plays the role of an integration, where for example,

$$\theta^{-1} q^m = \frac{q^m}{m} \quad (m \ge 1) , \qquad \theta^{-1} L^j = \frac{L^{j+1}}{j+1} ,$$

$$\theta^{-1}\left(q^m L^j\right) = \sum_{i=0}^{j} (-1)^i \, \frac{j!}{(j-i)!} \, \frac{q^m L^{j-i}}{m^{\,i+1}} \,. \tag{58}$$

We write the integration as θ^{-1} rather than as $\int dq/q$ for two reasons. First, θ^{-1} absorbs the measure, so that a letter is exactly what stands to the right of θ^2 in Eq. (56). Second, it replaces the regularization at the base point by the algebraic rule on the first line of Eq. (58). That regularization is needed because a letter with a constant term, such as $\zeta\,\psi_1\omega_0$ itself, makes $\int dq/q$ divergent at the base point. The rule is the analog of $\log^k x/k!$ for an ordinary polylogarithm. The definition of iterated integrals respects the shuffle product,

$$I(f_1,\ldots,f_m;q)\, I(f_{m+1},\ldots,f_{m+n};q) = \sum_{\sigma} I(f_{\sigma(1)},\ldots,f_{\sigma(m+n)};q)\,, \tag{59}$$

with the sum running over the $\binom{m+n}{m}$ interleavings of the two sequences that preserve the order within each. The length of the arguments is its transcendental weight. It is raised by one at every θ^{-1}, and L carries weight one by the same rule. Note that the modular weight in Eq. (53) is a different concept, attached to the letters alone. It restricts which kernels may appear, is not raised by integration, and does not enter the weight count of a function. For example, $I(1,\psi_1\omega_0,\omega_0,\omega_1,\omega_1;q)$ is a function of transcendental weight five, whose letters carry modular weights $0,3,2,2,2$.

As an example, take the transcendental weight-2 function that occurs below, $I(1,\psi_1\omega_0;q)$. By Eqs. (51) and (54) its letter is $\psi_1\omega_0 = \psi_1^3(1-\zeta)(1+8\zeta) = 1+q-5q^2+q^3+11q^4-24q^5+\ldots$. Because this letter has a constant term, the inner integration produces a power of L through the second rule of Eq. (58). The outer integration, against the constant letter 1, produces another:

$$\begin{aligned} I(\psi_1\omega_0;q) &= L + q - \frac{5}{2}q^2 + \frac{1}{3}q^3 + \frac{11}{4}q^4 - \frac{24}{5}q^5 + \ldots\,, \\ I(1,\psi_1\omega_0;q) &= \frac{L^2}{2} + q - \frac{5}{4}q^2 + \frac{1}{9}q^3 + \frac{11}{16}q^4 - \frac{24}{25}q^5 + \ldots\,, \end{aligned} \tag{60}$$

where the $L^2/2$ comes from $\theta^{-1}L$ and every q^m has been divided by m once more. For iterated Eisenstein integrals whose letters are only ω_0 and ω_1, the integral reduces to the usual GPLs (HPLs in this case). For example, $I(\omega_1;q) = H_1(\zeta) = -\log(1-\zeta)$.

Applying θ^{-1} twice and using iterated Eisenstein integrals, the analytic expression for S_0 is

$$\begin{aligned} \frac{S_0}{\psi_1} = {} & \frac{33}{4}\zeta_5 - \frac{1}{12}\pi^2\zeta_3 - \frac{1}{30}\pi^4 L - 4\,I(1,\zeta\psi_1\omega_0,\omega_0,\omega_0,\omega_1;q) - 4\,I(1,\zeta\psi_1\omega_0,\omega_0,\omega_1,\omega_1;q) \\ & - 4\,I(1,\zeta\psi_1\omega_0,\omega_1,\omega_0,\omega_1;q) - 4\,I(1,\zeta\psi_1\omega_0,\omega_1,\omega_1,\omega_1;q) - I(1,\psi_1\omega_0,\omega_0,\omega_0,\omega_1;q) \\ & - \frac{5}{2}\,I(1,\psi_1\omega_0,\omega_0,\omega_1,\omega_1;q) - \frac{7}{2}\,I(1,\psi_1\omega_0,\omega_1,\omega_0,\omega_1;q) - 5\,I(1,\psi_1\omega_0,\omega_1,\omega_1,\omega_1;q) \\ & - \frac{3}{2}\,I(1,\psi_1\omega_0,\omega_0,\omega_1,\omega_0;q) + \frac{3}{2}\,I(1,\psi_1\omega_0,\omega_1,\omega_0,\omega_0;q) - \frac{\pi^2}{4}\,I(1,\psi_1\omega_0,\omega_1;q) \end{aligned}$$

$$- 4\zeta_3\, I(1, \zeta\psi_1\omega_0; q) + \frac{1}{2}\zeta_3\, I(1, \psi_1\omega_0; q)\,, \tag{61}$$

where the first three terms are fixed by the boundary data. The boundary data are the value and the $\log\zeta$ coefficient of S_0 at $\zeta = 0$, read off the expansion of the two-fold integral of Eq. (34) at $\zeta = 0$. We can also obtain the analytic form for $S_0^{'}$ via

$$S_0' = \frac{\theta S_0}{\theta\zeta} = \frac{\theta S_0}{\psi_1^2\,\zeta(1-\zeta)(1+8\zeta)}\,. \tag{62}$$

Finally, the elliptic sector then follows from Eq. (45).

3. Numerical evaluations

In this subsection we describe how we evaluate the iterated Eisenstein integrals and F_{K_1} numerically to high precision. The method, truncated q-series with the regularization of Eq. (58), is the standard one for iterated integrals of modular forms [58, 60] and is implemented in GiNaC [39]; we spell out our implementation because the letters, the inversion $\zeta \mapsto q$ and the precision control are specific to this problem. To obtain the value at a point ζ_0, we need three things: the point q_0 with $\zeta(q_0) = \zeta_0$, the q-expansions of the letters to some order N, and the iterated integrals as truncated series.

We first determine q_0. On the physical line q is real with $0 < q < 1$, and there the map $q \mapsto \zeta(q)$ is increasing, because $\theta\zeta = \psi_1^2\,\zeta(1-\zeta)(1+8\zeta) > 0$ by Eq. (52). The equation $\zeta(q_0) = \zeta_0$ therefore has exactly one solution. Near the collinear limit it is given by the inverse of the first series in Eq. (51),

$$q = \zeta - 3\zeta^2 + 15\zeta^3 - 85\zeta^4 + 522\zeta^5 - \dots\,, \tag{63}$$

which converges for $|\zeta| < \frac{1}{8}$, the distance from $\zeta = 0$ to the cusp $\zeta = -\frac{1}{8}$. Beyond that radius we solve $\zeta(q) = \zeta_0$ on the truncated series of the eta quotient, by bisection on $0 < q < 1$ followed by Newton's method, and four Newton steps suffice. For example, at $\zeta_0 = \frac{3}{11}$ we find $q_0 \approx 0.1739$ and $L = \log q_0 \approx -1.7493$, and at $\zeta_0 = \frac{1}{2}$ we find $q_0 \approx 0.2724$.

Next come the letters. In Eq. (51) each η_d is $\tilde{q}^{\,d/24}$ times the product $\prod_{n\geq 1}\left(1-\tilde{q}^{\,dn}\right)$ with $\tilde{q} = -q$. The fractional powers of $\tilde{q}$ cancel in ψ_1, $1-\zeta$ and $1+8\zeta$, and they combine to the single factor $-\tilde{q} = q$ in ζ. Each quotient is therefore a product of truncated series and of inverses of truncated series, and ζ and ψ_1 come out through order q^N with integer coefficients. Then ω_0, ω_1, $\psi_1\omega_0$ and $\zeta\psi_1\omega_0$ follow from Eq. (54) by series multiplication. The identity $\theta\zeta = \psi_1^2\,\zeta(1-\zeta)(1+8\zeta)$ must hold order by order, and we use it as the check of the truncated series.

The iterated integrals are built from the inside out. The innermost letter is a truncated series, and θ^{-1} is applied to it. Each further step multiplies the current result by the next letter, truncates at q^N, and applies θ^{-1} again, term by term with Eq. (58): a term $q^m L^j$ with $m \geq 1$ returns the terms $q^m L^{j-i}$ with the rational coefficients written there, and a term L^j without q returns $L^{j+1}/(j+1)$. Each integral is therefore a polynomial in L whose coefficients are truncated q-series with rational coefficients. A power of L is created only when θ^{-1} meets a term without q, that is, only by the letters with a constant term, which are 1, ω_0 and $\psi_1\omega_0$. Integrals whose innermost letter is ω_1 or $\zeta\psi_1\omega_0$ contain no L at all, and the power of L in an integral is the length of its innermost run of letters with a constant term. In Eq. (61) the highest power is L^2, from $I(1,\psi_1\omega_0,\omega_1,\omega_0,\omega_0;q)$ and $I(1,\psi_1\omega_0;q)$. Substituting q_0 and $L=\log q_0$ gives S_0, and its derivative can also be calculated directly. Thus these three steps provide us the way to evaluate the elliptic functions. The polylogarithmic functions on the other hand, can be evaluated directly in ζ_0 with the standard tools [35, 72, 73]. This completes the evaluation of F_{K_1}.

The precision is controlled by two components. Rounding enters only at the end, when q_0, $L=\log q_0$, the constants π^2, ζ_3, π^4, ζ_5 and Ψ are substituted in floating point, and the working precision of that substitution can be set as high as needed. Truncating every series at q^N drops terms of order q_0^{N+1}. The letters are holomorphic modular forms, whose q-coefficients grow at most polynomially, and θ^{-1} only divides by powers of m, so the truncation error is a constant times q_0^N. The number of correct decimal digits after N terms, D, is then

$$D \simeq N \log_{10}\frac{1}{q_0} - 3\,, \tag{64}$$

and fifty digits need $N \simeq 53/\log_{10}(1/q_0)$ terms by this estimate. In practice about 75 terms are needed at $\zeta_0=\frac{3}{11}$ and about 106 at $\zeta_0=\frac{1}{2}$, since Eq. (64) is slightly optimistic at large N. We have checked our implementation against the GiNaC one [38] on a sample of the iterated integrals of Eq. (61).

C. Final result

Putting everything together, we now have the full analytic expression for EEC at NNLO in $\mathcal{N}=4$ SYM. We write F_{NNLO} as the sum of polylogarithmic and elliptic parts, $F_{\mathrm{NNLO}}(\zeta) = F_{\mathrm{P}}(\zeta) + F_{\mathrm{E}}(\zeta)$, where

$$\begin{aligned} F_{\mathrm{P}}(\zeta) &= F_{\mathrm{HPL}}(\zeta) + 2\,\Psi(\zeta) + P(\zeta)\,, \\ F_{\mathrm{E}}(\zeta) &= 2\left[c_1 S_0 + c_2 S_0'\right] = 2\,F_{K_1}(\zeta) - 2\,\Psi(\zeta)\,. \end{aligned} \tag{65}$$

with $F_{\rm HPL}(\zeta)$ provided by Ref. [1]. Here we use the HPLs with $\{0,+,-\}$ notations to express $F_{\rm P}(\zeta)$. Explicitly, these letters are

$$H_{a_1,\ldots,a_n}(\sqrt{\zeta}) = \int_0^{\sqrt{\zeta}} dt\, f_{a_1}(t)\, H_{a_2,\ldots,a_n}(t)\,, \qquad a_i \in \{0,+,-\}\,,$$
$$f_0(t) = \frac{1}{t}\,, \quad f_+(t) = \frac{1}{1-t} + \frac{1}{1+t} = \frac{2}{1-t^2}\,, \quad f_-(t) = \frac{1}{1-t} - \frac{1}{1+t} = \frac{2t}{1-t^2}\,. \tag{66}$$

We omit the $\sqrt{\zeta}$ argument in HPLs to save space and write $H_{a_1,\ldots,a_n} \equiv H_{a_1,\ldots,a_n}(\sqrt{\zeta})$ below. Then the full analytic expression of $F_{\rm P}(\zeta)$ is,

$$\begin{aligned}
F_{\rm P}(\zeta) &= (\zeta-1)\,\Big[-4\,H_{-,0,0} - 32\,H_{-,0,-,0} - 2\,H_{+,+,0,0} - 2\,H_{+,0,+,0,0} - 2\,H_{+,+,0,-,-}\Big] \\
&\quad - 8\,(\zeta+1)\;H_{-,0,0,-,0} + \sqrt{\zeta}\,(\zeta-1)\,\Big[4\,H_{0,+,0} + 6\,H_{-,+,0} + 4\,H_{+,0,0} + 8\,H_{+,0,-} - 6\,H_{+,-,0} \\
&\quad + 4\,H_{0,0,+,0} + 8\,H_{0,-,+,0} + 8\,H_{0,+,0,-} - 8\,H_{0,+,-,0} + 8\,H_{-,0,+,0} + 15\,H_{-,-,+,0} + 2\,H_{-,+,0,0} \\
&\quad + 16\,H_{-,+,0,-} - 15\,H_{-,+,-,0} - 32\,H_{+,0,0,-} + 32\,H_{+,0,-,0} - 2\,H_{+,-,0,0} - 16\,H_{+,-,0,-} \\
&\quad + 15\,H_{+,-,-,0} - 15\,H_{+,+,+,0} + \frac{1}{3}\pi^2\,H_+ + \frac{2}{3}\pi^2\,H_{0,+} + \frac{7}{6}\pi^2\,H_{-,+} - \frac{2}{3}\pi^2\,H_{+,0} - \frac{7}{6}\pi^2\,H_{+,-} \\
&\quad + \zeta_3\,H_+\Big] - \frac{1}{6}\,(\zeta-1)\,(\zeta-5)\,\pi^2\,H_{-,0} + \frac{1}{3}\,(\zeta-4)\,(\zeta-1)\,\zeta_3\,H_- - \left(\zeta^2-4\zeta-20\right)\,H_{-,-,-,0,-} \\
&\quad + \zeta\,(\zeta-3)\,\Big[-8\,H_{0,-,-,0,-} - 2\zeta_3\,H_{0,-}\Big] + (\zeta-1)\,(\zeta-2)\,\Big[-4\,H_{0,-,0,0} - 2\,H_{-,-,0,0}\Big] \\
&\quad + (\zeta-1)^2\,\Big[\frac{47}{3}\,H_{-,0,-,-} + 9\,H_{-,-,-,-} - \frac{1}{2}\zeta_3\,H_{+,+}\Big] + \zeta\,(\zeta-1)\,\Big[-16\,H_{0,0,-} + 16\,H_{0,-,0} \\
&\quad - 8\,H_{-,0,-} - 18\,H_{0,-,-,0} + 24\,H_{0,+,+,0} + 6\,H_{0,0,-,-,0} - \frac{2}{3}\pi^2\,H_0 - \frac{1}{3}\pi^2\,H_- + \pi^2\,H_{0,0} \\
&\quad + \frac{1}{3}\pi^2\,H_{+,+,0} + 2\zeta_3\Big] + (\zeta-1)\,(\zeta+1)\,\Big[-4\,H_{+,0,+,0} - 8\,H_{+,+,0,-} - 2\,H_{+,0,0,+,0} \\
&\quad - 4\,H_{+,0,+,0,-}\Big] + \zeta^2\,\Big[24\,H_{0,-,0,-,-} - \pi^2\,H_{0,-,0}\Big] + \zeta\,(\zeta+1)\,\Big[-4\zeta_3\,H_{0,0} + \frac{1}{6}\pi^2\zeta_3\Big] \\
&\quad + (\zeta-1)\,(\zeta+3)\,\Big[H_{-,+,+,0,0} - H_{+,-,+,0,0} + H_{+,+,-,0,0} - \frac{1}{3}\pi^2\,H_{-,0,0}\Big] \\
&\quad + \left(\zeta^2+4\zeta-3\right)\,\Big[-2\,H_{-,0,-,0,0} - H_{-,-,-,0,0}\Big] + 4\zeta\,(\zeta+6)\;H_{0,0,-,0,-} \\
&\quad - \left(\zeta^2+8\zeta+1\right)\,H_{-,0,-,-,0} - (\zeta-1)\,(\zeta+14)\;H_{-,-,-,0} - 4\left(2\zeta^2-\zeta-7\right)\,H_{-,-,0,0,-} \\
&\quad + (\zeta-1)\,(2\zeta+1)\,\Big[-2\,H_{+,+,0} + 8\,H_{+,+,0,0,-} - \frac{1}{6}\pi^2\,H_{+,0,+}\Big] + 3\left(2\zeta^2+3\right)\,H_{-,-,-,-,-} \\
&\quad - \left(3\zeta^2-2\zeta-13\right)\,H_{-,0,+,+,0} + 8\zeta\,(3\zeta-2)\;H_{0,0,0,0,-} + \zeta\,(3\zeta-1)\,\Big[4\,H_{0,+,0,+,0} + 8\,H_{0,+,+,0,-}\Big] \\
&\quad - \frac{1}{180}\,(\zeta-1)\,(3\zeta+4)\,\pi^4 + 2\zeta\,(3\zeta+1)\;H_{0,+,+,0,0} + 2\left(4\zeta^2-6\zeta+7\right)\,H_{-,0,0,-,-} \\
&\quad + 2\,(\zeta-1)\,(4\zeta-1)\;H_{-,-,0} + 4\left(4\zeta^2-4\zeta+9\right)\,H_{-,0,0,0,-} - 8\,(\zeta-1)\,(4\zeta+1)\;H_{0,0,-,0} \\
&\quad + 8\zeta\,(4\zeta-3)\;H_{0,0,0,-,0} - \frac{1}{6}\left(4\zeta^2-2\zeta+3\right)\pi^2\,H_{-,-,0} + (\zeta-1)\,(4\zeta+3)\,\Big[H_{-,+,0,+,0} \\
&\quad + 2\,H_{-,+,+,0,-} - H_{+,0,-,+,0} + H_{+,0,+,-,0} - H_{+,-,0,+,0} - 2\,H_{+,-,+,0,-} - 4\,H_{+,+,0,-,0}
\end{aligned}$$

$$
\begin{aligned}
&+ 2\,H_{+,+,-,0,-} - \frac{1}{6}\pi^2\,H_{+,+}\Big] + \left(4\zeta^2-\zeta+15\right)\,H_{-,0,-,-,-} + 2\left(4\zeta^2+\zeta+17\right)\,H_{-,0,-,0,-}\\
&+ \frac{1}{2}\left(4\zeta^2+6\zeta+3\right)\zeta_3\,H_{-,-} + \left(4\zeta^2+7\zeta-12\right)\zeta_3\,H_{-,0} - 4\zeta\,(5\zeta-9)\,H_{0,-,0,0,-}\\
&+ \frac{1}{6}\,(\zeta-1)\,(5\zeta+2)\,\pi^2\,H_{-,-} + \zeta\,(5\zeta-3)\,\Big[-4\,H_{0,0,-,0,0} - 2\,H_{0,-,-,0,0}\Big]\\
&+ (\zeta-1)\,(5\zeta+3)\,\Big[-\frac{3}{2}\,H_{-,-,+,+,0} + \frac{3}{2}\,H_{-,+,-,+,0} - \frac{3}{2}\,H_{-,+,+,-,0} - \frac{3}{2}\,H_{+,-,-,+,0}\\
&+ \frac{3}{2}\,H_{+,-,+,-,0} - \frac{3}{2}\,H_{+,+,-,-,0} + \frac{3}{2}\,H_{+,+,+,+,0}\Big] + 2\zeta\,(5\zeta+3)\,H_{0,0,-,-,-}\\
&+ \frac{1}{3}\,(\zeta-1)\,(7\zeta-1)\,\pi^2\,H_{0,-} + 4\zeta\,(7\zeta-5)\,H_{0,0,0,-,-} + (\zeta-1)\,(7\zeta+3)\,\Big[\frac{1}{12}\pi^2\,H_{-,+,+}\\
&- \frac{1}{12}\pi^2\,H_{+,-,+} + \frac{1}{12}\pi^2\,H_{+,+,-}\Big] + \zeta\,(7\zeta-3)\,\Big[-3\,H_{0,-,+,+,0} + 3\,H_{0,+,-,+,0} - 3\,H_{0,+,+,-,0}\Big]\\
&+ \frac{1}{90}\zeta\,(7\zeta+12)\,\pi^4\,H_0 - \frac{1}{12}\,(2\zeta-1)\,(4\zeta+1)\,\pi^2\,H_{-,-,-} - \frac{1}{6}\,(\zeta+1)\,(8\zeta-9)\,\pi^2\,H_{-,0,-}\\
&+ (\zeta-1)\,(8\zeta+7)\,\Big[H_{-,+,+,0} - H_{+,-,+,0} + H_{+,+,-,0}\Big] + 2\,(\zeta-1)\,(9\zeta-1)\,H_{-,-,0,-}\\
&+ \zeta\,(9\zeta-5)\,\Big[\frac{1}{6}\pi^2\,H_{0,+,+} - 2H_{0,0,+,+,0}\Big] - \frac{1}{3}\zeta\,(9\zeta-4)\,\pi^2\,H_{0,0,-}\\
&+ \left(9\zeta^2-2\zeta+12\right)\,H_{-,-,0,-,-} - \frac{1}{6}\zeta\,(9\zeta+1)\,\pi^2\,H_{0,-,-} - \frac{1}{720}\left(11\zeta^2+27\zeta-45\right)\pi^4\,H_-\\
&- \frac{2}{3}\,(\zeta-1)\,(13\zeta-1)\,\zeta_3\,H_0 + 2\left(13\zeta^2-4\zeta-2\right)\,H_{-,-,0,-,0} + \zeta\,(13\zeta+3)\,H_{0,-,-,-,-}\\
&+ 4\zeta\,(17\zeta-9)\,H_{0,-,0,-,0} - \frac{1}{4}\zeta\,(17\zeta+60)\,\zeta_5 + \frac{2}{3}\,(\zeta-1)\,(19\zeta-10)\,H_{0,-,-,-}\\
&+ \frac{1}{2}\left(25\zeta^2-12\zeta-1\right)\,H_{-,-,-,-,0} + \zeta\,(29\zeta-15)\,H_{0,-,-,-,0} + \frac{2}{3}\,(\zeta-1)\,(31\zeta-10)\,H_{0,0,-,-}\\
&+ \frac{4}{3}\,(\zeta-1)\,(31\zeta-7)\,H_{0,-,0,-} + \frac{2}{3}\,(\zeta-1)\,(47\zeta+1)\,H_{-,0,0,-} + \frac{4}{3}\,(\zeta-1)\,(55\zeta-4)\,H_{0,0,0,-}\,.
\end{aligned}
\tag{67}
$$

For the elliptic part, we write

$$
F_{\rm E}(\zeta) = 2A(\zeta)\,\frac{S_0}{\psi_1} + 2B(\zeta)\,\theta\left(\frac{S_0}{\psi_1}\right)\,, \tag{68}
$$

with the coefficients

$$
\begin{aligned}
A(\zeta) &= \frac{\zeta\,(\zeta-1)\,(8\zeta-5)}{3}\,\psi_1(\zeta) + \frac{\zeta\,(\zeta-1)^2\,(8\zeta+1)}{3}\,\psi_1'(\zeta)\,,\\
B(\zeta) &= \frac{c_2}{\psi_1\,\zeta(1-\zeta)(1+8\zeta)} = \frac{1-\zeta}{3\,\psi_1(\zeta)}\,,
\end{aligned}
\tag{69}
$$

These coefficients contain ψ_1 and its derivative,

$$
\psi_1'(\zeta) = \frac{d\psi_1}{d\zeta} = \sum_{n\geq 1}(-1)^n\,n\Big[\sum_{k=0}^{n}\binom{n}{k}^3\Big]\zeta^{n-1} = -2 + 20\zeta - 168\zeta^2 + 1384\zeta^3 - \dots\,. \tag{70}
$$

The transcendental part S_0/ψ_1 is given in Eq. (61), and its derivative $\theta\,(S_0/\psi_1)$ is,

$$
\theta\left(\frac{S_0}{\psi_1}\right) = -\frac{1}{30}\pi^4 - 4\,I(\zeta\psi_1\omega_0,\omega_0,\omega_0,\omega_1;q) - 4\,I(\zeta\psi_1\omega_0,\omega_0,\omega_1,\omega_1;q) - 4\,I(\zeta\psi_1\omega_0,\omega_1,\omega_0,\omega_1;q)
$$

$$
\begin{aligned}
&- 4\,I(\zeta\psi_1\omega_0,\omega_1,\omega_1,\omega_1;q) - I(\psi_1\omega_0,\omega_0,\omega_0,\omega_1;q) - \frac{5}{2}\,I(\psi_1\omega_0,\omega_0,\omega_1,\omega_1;q)\\
&- \frac{7}{2}\,I(\psi_1\omega_0,\omega_1,\omega_0,\omega_1;q) - 5\,I(\psi_1\omega_0,\omega_1,\omega_1,\omega_1;q) - \frac{3}{2}\,I(\psi_1\omega_0,\omega_0,\omega_1,\omega_0;q)\\
&+ \frac{3}{2}\,I(\psi_1\omega_0,\omega_1,\omega_0,\omega_0;q) - \frac{\pi^2}{4}\,I(\psi_1\omega_0,\omega_1;q) - 4\zeta_3\,I(\zeta\psi_1\omega_0;q) + \frac{\zeta_3}{2}\,I(\psi_1\omega_0;q)\,. \qquad (71)
\end{aligned}
$$

Using the analytic form, we can also obtain the asymptotic expansions to very high powers in both collinear and back-to-back limits. Explicitly, in the collinear limit, we find

$$
\begin{aligned}
F_{\rm NNLO}(\zeta) = {}& \zeta\Big[\frac{1}{2}\log^2\zeta + \left(-5+\frac{\pi^2}{3}-\zeta_3\right)\log\zeta + 17 - \frac{4\pi^2}{3} - \zeta_3 + \frac{5\pi^4}{144} + \frac{3\zeta_5}{2}\Big]\\
&+ \zeta^2\Big[\left(\frac{349}{144}+\frac{5\pi^2}{48}-3\zeta_3\right)\log^2\zeta + \left(-\frac{6569}{432}-\frac{121\pi^2}{144}-\frac{19\zeta_3}{2}+\frac{67\pi^4}{180}\right)\log\zeta\\
&\quad + \frac{16361}{864}+\frac{649\pi^2}{288}-\frac{7\zeta_3}{12}+\frac{511\pi^4}{1440}+\pi^2\zeta_3-\frac{347\zeta_5}{4}\Big]\\
&+ \zeta^3\Big[\left(-\frac{560707}{43200}-\frac{\pi^2}{24}+11\zeta_3\right)\log^2\zeta + \left(\frac{7234927}{72000}-\frac{13\pi^2}{90}+\frac{149\zeta_3}{4}-\frac{22\pi^4}{15}\right)\log\zeta\\
&- \frac{2555783}{11250}+\frac{148123\pi^2}{32400}+\frac{24107\zeta_3}{360}-\frac{3427\pi^4}{1440}-\frac{11\pi^2\zeta_3}{3}+363\zeta_5\Big] + \mathcal{O}\left(\zeta^4\right)\,. \qquad (72)
\end{aligned}
$$

In the back-to-back limit, we also define $y \equiv 1-\zeta$ and the asymptotic expansion reads

$$
\begin{aligned}
F_{\rm NNLO}(\zeta) = {}& \Big[-\frac{1}{8}\log^5 y - \frac{\pi^2}{6}\log^3 y - \frac{11\zeta_3}{4}\log^2 y - \frac{61\pi^4}{720}\log y - \frac{\pi^2\zeta_3}{3} - \frac{7\zeta_5}{2}\Big]\\
&+ y\Big[\frac{1}{10}\log^5 y - \frac{1}{3}\log^4 y + \left(-\frac{1}{6}+\frac{5\pi^2}{72}\right)\log^3 y + \left(\frac{1}{4}-\frac{3\pi^2}{8}+2\zeta_3\right)\log^2 y\\
&+ \left(-2-\frac{\pi^2}{6}-3\zeta_3-\frac{5\pi^4}{72}\right)\log y + 14 + \frac{13\pi^2}{12} - 3\pi^2\log 2 - \zeta_3 - \frac{173\pi^4}{360}\\
&+ 2\pi^2\log^2 2 + \log^4 2 + 24\,{\rm Li}_4\left(\frac{1}{2}\right) + \frac{247\pi^4\log 2}{240} - \frac{8\pi^2\log^3 2}{3} - \frac{11\pi^2\zeta_3}{24}\\
&- \frac{4\log^5 2}{5} - \frac{2917\zeta_5}{32} + 96\,{\rm Li}_5\left(\frac{1}{2}\right) - 2S_0(1)\Big]\\
&+ y^2\Big[-\frac{1}{20}\log^5 y + \frac{13}{16}\log^4 y + \left(-\frac{97}{24}-\frac{\pi^2}{72}\right)\log^3 y + \left(\frac{431}{32}+\frac{9\pi^2}{16}-\frac{3\zeta_3}{4}\right)\log^2 y\\
&+ \left(-\frac{275}{8}-\frac{43\pi^2}{24}+9\zeta_3+\frac{5\pi^4}{72}\right)\log y + \frac{705}{16}+\frac{113\pi^2}{96}+\frac{9\pi^2\log 2}{4}-\frac{105\zeta_3}{4}\\
&+ \frac{947\pi^4}{2880} - \frac{7\pi^2\log^2 2}{3} - \frac{7\log^4 2}{6} - 28\,{\rm Li}_4\left(\frac{1}{2}\right) - \frac{2\pi^4\log 2}{3} + \frac{5\pi^2\log^3 2}{3}\\
&+ \frac{17\pi^2\zeta_3}{16} + \frac{\log^5 2}{2} + \frac{941\zeta_5}{16} - 60\,{\rm Li}_5\left(\frac{1}{2}\right) + 2S_0(1)\Big] + \mathcal{O}\left(y^3\right)\,, \qquad (73)
\end{aligned}
$$

where

$$
S_0(1) = \frac{611\sqrt{3}\,\pi^5}{19440} - 3\sqrt{3}\,{\rm Im}\,G\left(e^{-i\pi/3},0,0,0,1;1\right) \approx 13.804641453635316796566161 7535\,. \qquad (74)
$$

While the collinear expansion only contains zeta values, the back-to-back expansion requires $\log 2$, ${\rm Li}_n\,(1/2)$ and a special GPL. In Fig. 1, we show the comparisons of both expansions with the pure

NNLO (denoted as δNNLO). We keep both expansions up to the third order, namely $\mathcal{O}(\zeta^3)$ in the collinear limit and $\mathcal{O}((1-\zeta)^2)$ in the back-to-back limit. We observe that the collinear expansion provides a reliable prediction even at $\zeta \approx 0.5$.

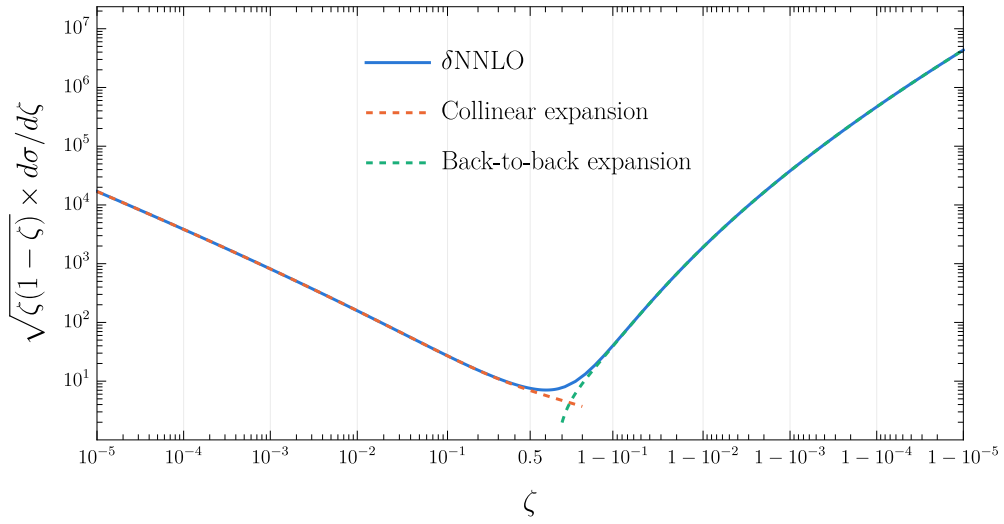

FIG. 1. Comparison of pure NNLO prediction δNNLO and its singular expansions in both the collinear and the back-to-back limits. The distribution is multiplied by $\sqrt{\zeta(1-\zeta)}$.

In Fig. 2, we show the fixed-order distribution of EEC up to NNLO, with $a = N_c g_{\rm YM}^2/(4\pi^2) = 0.09$ as an example. Unlike Fig. 1, here NLO includes up to $\mathcal{O}(a^2)$ contribution and NNLO includes up to $\mathcal{O}(a^3)$ contribution. In the bulk region, the order-by-order convergence is good, and the fixed-order predictions provided in the work are reliable. At both collinear and back-to-back endpoints, the distribution receives large logarithmic enhancements, so we observe instability across orders. In particular, the NLO curve goes negative around $1-\zeta \sim 10^{-2}$. Systematic resummation of these large logarithms is required at both endpoints to obtain reliable predictions.

V. A FIRST LOOK AT EEC BOOTSTRAP

We obtained the analytic $F_{\rm NNLO}$ from direct calculation by integrating the polylogarithmic sector directly and by solving the differential system of the elliptic sector. With the answer known, we can ask how much of it a Landau bootstrap in the sense of Ref. [74] would have fixed from the alphabet, the elliptic curve and the known limits alone. Such an analysis will benefit the EEC results in QCD at this order, where the integrand is known but the integrals are not.

The idea of perturbative bootstrap programs is to construct the transcendental function space

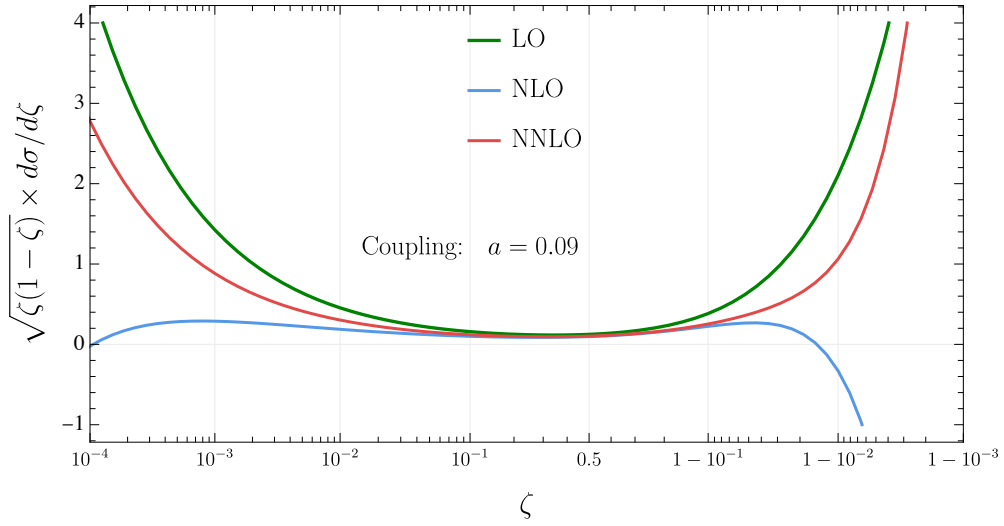

FIG. 2. Fixed-order prediction for EEC up to NNLO. Here we choose the coupling value $a = 0.09$.

from singularities, write down the ansatz for all rational coefficients, and determine the unknown parameters from either physical constraints or numerical data. For scattering amplitudes in planar $\mathcal{N} = 4$ SYM, the coefficients associated with the transcendental basis are rational numbers instead of functions, and there is enough physical information to fix them. For QCD observables with less symmetry, one can perform analytic regressions from high-precision numerical data, such as the lattice reduction approach developed in Ref. [55] and its application to the three-point energy correlators [75]. As we learn from Sec. IV C, EEC up to NNLO requires both polylogarithmic and elliptic sectors. In both cases, we need to determine the alphabets, all integrable symbols, and the candidate function space. Then we also need to make a reasonable ansatz for rational coefficients and determine what EEC properties we can make use of.

A. Alphabet and function space

A perturbative bootstrap program starts with the alphabet. For standard Feynman integrals, Landau analysis uses the analytic structures in the integrand, like branch cuts and singularities, and provides a sufficient set of letters. Algorithms are developed and implemented in PLD [76] and SOFIA [77]. For observables like differential cross-section, due to the on-shell constraints from phase space integrals, there is no canonical method to determine the alphabet. For EEC in $\mathcal{N} = 4$ SYM, we can learn the potential letters from the four-point correlator, whose discontinuity leads to our EEC integrand. Note that the four-point correlator carries the elementary letters z, $\bar{z}$, $1-z$

and $1-\bar{z}$, and its rational prefactor carries the denominator $z-\bar{z}$. Applying Eq. (9) and the rescaling $x = t/\bar{z}$, all of them will become polynomials in x of degree at most two over the common denominator D: z gives $x(x-1)$, while $1-z$, $z-\bar{z}$, $1-z-\bar{z}$ and $1-z\bar{z}$ give D_0, C, D_1 and D_2, with

$$C = \zeta x^2 + (\bar{z} - 2\zeta)\, x + \zeta - 1\,, \tag{75}$$

and other expressions in Eq. (11). The inner integration over $x \in [0,1]$ then produces logarithms whose arguments are cross ratios of the roots of these polynomials with the two endpoints $x = 0, 1$, carrying the square root of a discriminant whenever the two roots do not separate rationally. The outer integration over $\bar{z}$ produces the letters in ζ: they are the values the $\bar{z}$-dependent letters take at $\bar{z} = 0$ and $\bar{z} = 1$.

The map itself gives $\log(-z) = \log\zeta + \log\bar{z} + \log x + \log(1-x) - \log D$, whose only ζ letter is $\log\zeta$. The linear factor D has the single root $x_D = (\zeta-1)/(\zeta-\bar{z})$. After the x-integration a root enters only through its cross ratio with the endpoints $x = 0, 1$, here $x_D/(x_D-1) = (\zeta-1)/(\bar{z}-1)$, so D contributes the letters $1-\zeta$ and $1-\bar{z}$ and, at the outer endpoint $\bar{z} = 0$, only $1-\zeta$. The rational factor of D_0 returns the same letter. The first nontrivial object is C, and its discriminant is a conic in the outer variable,

$$R(\bar{z};\zeta) = \mathrm{disc}_x\, C = \bar{z}^2 - 4\zeta\bar{z} + 4\zeta\,, \qquad \mathrm{disc}_{\bar{z}}\, R = 16\zeta\,(\zeta-1)\,. \tag{76}$$

The x-integration puts $\sqrt{R(\bar{z};\zeta)}$ inside the $\bar{z}$-letters through the roots $x_\pm = (2\zeta - \bar{z} \pm \sqrt{R})/(2\zeta)$, and the $\bar{z}$-integration evaluates those letters at its endpoints, so the only algebraic quantities that can survive in ζ are $\sqrt{R(1;\zeta)} = 1$ and $\sqrt{R(0;\zeta)} = 2\sqrt{\zeta}$. At $\bar{z} = 1$ the discriminant is a perfect square, C factors rationally, and that endpoint returns nothing new. However, at $\bar{z} = 0$, it becomes $\zeta(x-1)^2 - 1$, with roots $1 \pm 1/\sqrt{\zeta}$. Their cross ratio with the endpoints of the x integration is the third letter,

$$\int_0^1 \frac{dx}{C(x,0;\zeta)} = \frac{1}{2\sqrt{\zeta}} \log\frac{1-\sqrt{\zeta}}{1+\sqrt{\zeta}}\,. \tag{77}$$

Putting these together, we conclude the polylogarithmic alphabet is

$$\mathcal{A}_{\mathrm{P}} = \left\{\zeta,\, 1-\zeta,\, \frac{1-\sqrt{\zeta}}{1+\sqrt{\zeta}}\right\}. \tag{78}$$

We emphasize that $z-\bar{z}$ only shows up in the prefactor of four-point correlator, not in the arguments of transcendental functions. The lesson we learn from this example is that one should always include the rational factors in the potential alphabet for safety.

With the alphabet at hand, we can construct the function space with polylogarithmic functions. Since we have one square root in the alphabet, it is better to introduce $\rho \equiv \sqrt{\zeta}$ and the letters become $\{\rho, 1-\rho, 1+\rho\}$. In general cases, one writes down all possible symbols up to a certain weight, with entries from the alphabet, and applies the integrability condition. The resulting symbol basis can then be lifted to polylogarithmic functions. In this case, since it is single variable, the integrability condition, first-entry condition or any Steinmann-type relations used in the amplitude bootstrap place no constraints. And with arguments $0, \pm 1$, the final function type is simply HPL. The discrete symmetry remains in the function space. Under the transformation $\rho \to -\rho$ the one-forms $f_0\, d\rho$ and $f_-\, d\rho$ of Eq. (66) are even and $f_+\, d\rho$ is odd, so a basis function is even or odd according to the parity of the number of + letters it contains. The observable is a function of $\zeta = \rho^2$ and must be invariant, so an odd basis function may appear only against an odd power of ρ. HPLs of ζ itself lie in the same space, through $H_u(\zeta) = 2^{\,n_0(u)} H_{u'}(\sqrt{\zeta})$ with $0 \to 0$, $1 \to -$ and $n_0(u)$ the number of zeros in u.

The elliptic side begins from the same integrand. The two quadratics D_1 and D_2 of Eq. (11) have discriminants Q_1 and Q_2 that are quartic in the outer variable, Eq. (20), and a quartic square root cannot be rationalized: the outer integration of a function containing $\sqrt{Q_i(\bar{z})}$ is a period integral on a curve of genus one. As discussed above, the two curves are the same by the Möbius relation of Eq. (21), and the family degenerates where the quartic acquires a double root, which by $\mathrm{disc}_{\bar{z}}\, Q_1 = \mathrm{disc}_{\bar{z}}\, Q_2 = 256\, \zeta^6 (1-\zeta)^2 (1+8\zeta)$ happens at $\zeta = 0, 1, -\frac{1}{8}, \infty$. Four maximally unipotent singular fibers identify the family as the equal-mass sunrise family with modular group $\Gamma_1(6)$, as Sec. III shows independently by comparing j-invariants, and the cusp widths 1, 2, 3 and 6 sum to the index 12. All these properties follow from the NNLO integrand, and it is also why the elliptic sector only starts at this order.

The elliptic letters then follow from the geometry together with the same physical-singularity rule that fixed Eq. (78). A logarithmic letter ℓ contributes the kernel $\theta \log \ell = (\theta\zeta)\, d\log \ell / d\zeta$, and by Eq. (52) the factor $\theta\zeta = \psi_1^2 \zeta(1-\zeta)(1+8\zeta)$ carries $1+8\zeta$. Since $d\log\ell/d\zeta$ may be singular only at the physical points $\zeta = 0$ and $\zeta = 1$, nothing can cancel that factor and it survives in every admissible letter. At modular weight two this gives

$$\psi_1^2\,(1+8\zeta) \cdot \mathrm{span}_{\mathbb{Q}}\,\{1, \zeta\} = \mathrm{span}_{\mathbb{Q}}\,\{\omega_0, \omega_1\}\ , \tag{79}$$

a two-dimensional subspace of the three-dimensional M_2 of Eq. (53). At modular weight three the letter is the one left behind by variation of parameters. Writing $S_0 = \psi_1 g$ and using $L_{\mathrm{PF}}\psi_1 = 0$, the second-order operator collapses to two antiderivatives, $\theta^2 g = -\psi_1^3 \zeta(1-\zeta)(1+8\zeta)\, J$ with J the

source of the inhomogeneous Picard–Fuchs equation for S_0. We do not have access to the source from the bootstrap perspective; however, there are two properties we can use: it is a polylogarithm in ζ over the letters ζ and $1-\zeta$ with rational coefficients, and its weight is at most three. Therefore an admissible kernel is $\psi_1^3\zeta(1-\zeta)(1+8\zeta)\,r(\zeta)$ with r rational and singular only at $\zeta = 0, 1$. Requiring it to be a holomorphic modular form of weight three, that is ψ_1^3 times a polynomial of degree at most three, bounds the pole orders with no further assumption. This leaves

$$\mathcal{A}^{(3)} = \psi_1^3\,(1+8\zeta)\cdot \mathrm{span}_{\mathbb{Q}}\left\{1, \zeta, \zeta^2\right\}\,, \tag{80}$$

three-dimensional inside the four-dimensional M_3. Together with the constant letter, which the outer integration requires, the elliptic alphabet is

$$\mathcal{A}_{\mathrm{E}} = \{1\} \cup \{\omega_0, \omega_1\} \cup \mathcal{A}^{(3)}\,. \tag{81}$$

In the NNLO bootstrap below, as a robustness test, we will directly build the ansatz on all of M_3 and M_2, and we will see the resulting solution confirm this alphabet.

The alphabet fixes the kernels, and the operator θ fixes the order of iteration. The iterated integrals are $I(f_1, \ldots, f_n; q) = \theta^{-1}[f_1\, I(f_2, \ldots, f_n; q)]$ with the leftmost entry outermost. The elliptic function to be constructed is $g = S_0/\psi_1$, and by the variation of parameters above it is a double antiderivative, $g = \theta^{-2}[f\,J]$ up to solutions of $\theta^2 g = 0$, of the kernel $f = -\zeta\,\psi_1\omega_0 \in \mathcal{A}^{(3)}$ times the source J, the polylogarithm of weight at most three over the letters ζ and $1-\zeta$ characterized above.

Every iterated integral in g therefore has the constant 1 as its outermost kernel. Then we have exactly one weight-three kernel as its second entry, and after that only ω_0 and ω_1, which are the one-forms $d\log\zeta$ and $-d\log(1-\zeta)$ of the polylogarithms inside the source written in the variable $\log q$. Differentiation respects the order of iteration. A weight-5 solution takes the form

$$g = c_0 + c_L L + \sum_{f\in\mathcal{A}^{(3)}} \Big[\sum_{|u|=3} a_{fu}\, I(1, f, \omega_{u_1}, \omega_{u_2}, \omega_{u_3}; q) + \pi^2 \sum_{|u|=1} b_{fu}\, I(1, f, \omega_{u_1}; q) + \zeta_3\, d_f\, I(1, f; q)\Big]\,, \tag{82}$$

with $u = u_1 \cdots u_{|u|}$ a string of indices in $\{0, 1\}$, rational coefficients a, b, d, and the transcendental constants written as $c_0 = c_5\zeta_5 + c_{23}\pi^2\zeta_3$, $c_L = c_4\pi^4$.

B. Rational coefficients ansatz

What makes a bootstrap program for observables or cross-sections challenging is the rational coefficients. For amplitudes in planar $\mathcal{N} = 4$ SYM the coefficient of each transcendental function is

a rational number, and thus the whole content of the ansatz is the function list. Here the coefficients are rational functions of ζ, so a second assumption is needed and the number of unknown parameters is dominated by it. We take the shape proposed for the three-point correlator in Ref. [75], in which the denominator is built from the rational letters of the alphabet with the pole orders left as parameters and the numerator degree tied to them.

Write $\rho = \sqrt{\zeta}$, let T run over the basis of total weight at most $2n-1$ and let $p(T) \in \{0,1\}$ be the parity of the type in the sense of Sec. V A. Allowing a pole of order m_0 at $\zeta = 0$ and m_1 at $\zeta = 1$, the ansatz is

$$F^{(n)}(\zeta) = \frac{1}{\zeta^{\,m_0}\,(1-\zeta)^{m_1}} \sum_T \rho^{\,p(T)} \Big[\sum_{j=0}^{d-p(T)} c_{T,j}\, \zeta^{\,j} \Big]\, T(\rho)\,, \qquad d \geq 2 + m_0 + m_1\,, \tag{83}$$

with the unknown rational coefficients $c_{T,j}$. The factor $\rho^{\,p(T)}$ is forced by the parity transformation which makes every term invariant under $\rho \to -\rho$, so that the expansion at $\zeta = 0$ runs in integer powers of ζ alone. Tying the numerator degree to the pole orders by $d = 2 + m_0 + m_1$ fixes the polynomial part of each coefficient, after partial fractioning, to degree two in ζ on the even types and to ρ times degree one on the odd ones. Both $m_{0,1}$ and d can be increased in the ansatz, and the final answer should remain the same after imposing the constraints. This also serves as a consistency check. Note that for the three-point correlator, the leading transcendentality is computed through the spherical contour method and thus one has a sense of how the rational coefficients should look at lower transcendentality. Here we propose the form of Eq. (83) for every basis function.

The elliptic sector needs the same treatment. Section V A constructed $g = S_0/\psi_1$ as a combination $\sum_w a_w\, I(w;q)$ of the iterated integrals of Eq. (82) with rational numbers a_w, plus the homogeneous terms. What enters the correlator is not $S_0 = \psi_1 g$ by itself: the elliptic part of the observable is a combination of S_0 and its first derivative with rational-function coefficients, $F_{\rm E} = 2\,[c_1(\zeta) S_0 + c_2(\zeta) S_0']$ (Sec. IV C), and no higher derivative can occur because the Picard-Fuchs equation is of second order. A bootstrap knows neither c_1, c_2 nor the a_w. Substituting $S_0 = \psi_1 \sum_w a_w I(w;q)$ shows what it must parametrize: every iterated integral $\psi_1 I(w;q)$ and its ζ-derivative, each with an unknown rational function in front. The general linear ansatz for the elliptic sector is therefore

$$F_{\rm E}(\zeta) = \sum_w \left[r_w(\zeta)\, \psi_1\, I(w;q) + s_w(\zeta)\, \frac{d}{d\zeta}\Big(\psi_1\, I(w;q)\Big) \right], \tag{84}$$

with r_w and s_w rational functions of the shape (83), poles at $\zeta = 0, 1$, chosen independently for every iterated integral.

C. Physical and numerical constraints

In this subsection, we describe the physical constraints that we will use to determine the unknown parameters in the bootstrap. They are most transparent on the EEC distribution $d\sigma/d\zeta$ and can be translated to F. Since $F = 2\zeta^2(1-\zeta)\, d\sigma/d\zeta$, a term $f_{k,j}\zeta^k \log^j \zeta$ of F contributes to $d\sigma/d\zeta$ at order ζ^{k-2}, and with $y = 1-\zeta$ a term $b_{k,j} y^k \log^j y$ contributes at order y^{k-1}. Every condition below is imposed channel by channel: the unknown parameters are rational numbers, so we equate the coefficients of 1, π^2, ζ_3, π^4, ζ_5 and $\pi^2\zeta_3$ separately. We list the conditions in the order of what they require.

(C1) Regularity. The cross section diverges no faster than $1/\zeta$ in the collinear limit and no faster than $1/y$ in the back-to-back limit, which bounds the powers in F. The logarithms are bounded by the loop order: the collinear expansion is a single-logarithm series in $a\log\zeta$, so at order a^n it carries at most $\log^{n-1}\zeta$, and the back-to-back expansion is a double-logarithm series, so at order a^n it carries at most $\log^{2n-1} y$. These properties are purely from our understanding of soft and collinear divergences, and we impose them in the endpoint expansion.

A further condition of the same kind is that the local exponents at both endpoints are integers: both expansions of $d\sigma/d\zeta$ run in integer powers of the local variable times logarithms. On the polylogarithmic ansatz this is automatic once the parity in ρ is built in. It matters when the elliptic sector is written on a system larger than the Picard-Fuchs operator: the coupled system in Eq. (44) has four homogeneous solutions, and the two that are not periods behave as $y^{\pm\sqrt{5/3}}$ at $\zeta = 1$. Requiring integer exponents removes these two solutions and thereby selects the physical combination, without using the fact that the system in Eq. (44) eventually decouples. It is this requirement that forces the function Ψ of Eq. (48) to be a polylogarithm. The elliptic ansatz in Eq. (84) satisfies the requirement automatically: ψ_1 and the factors ζ, $1-\zeta$ and $1+8\zeta$ of Eq. (51) are eta quotients, which vanish to integer order at each of the four cusps, so every term of the ansatz has integer local exponents there, up to powers of logarithms.

(C2) Collinear leading power. As $\zeta \to 0$ the light-ray operator product expansion [11, 12] organizes $d\sigma/d\zeta$ in powers of ζ labeled by the twist of the exchanged light-ray operators. The leading twist-two term is $1/\zeta$ times a series in a and $\log\zeta$ that exponentiates to a power of ζ set by twist-two anomalous dimensions. Expanding to order a^n, it is $1/\zeta$ times a polynomial in $\log\zeta$ of degree $n-1$ with predicted coefficients. In F this is the ζ^1 bracket, $F^{(n)} = \zeta\sum_{j<n} c_{nj}\log^j\zeta + \mathcal{O}(\zeta^2)$, at NNLO the first line of Eq. (72). In QCD the same information comes from the collinear factorization theorem [10].

(C3) Back-to-back leading power. As $\zeta \to 1$ the distribution is a Sudakov form factor: $d\sigma/d\zeta$ is $1/y$ times a double-logarithmic series whose coefficients follow from effective field theory predictions [12, 17], at order a^n a polynomial in $\log y$ of degree $2n-1$. In F this is the y^0 bracket, at NNLO the first line of Eq. (73). Its constants are multiple zeta values and contain no $\log 2$.

Condition (C3) contains a second requirement that is easy to overlook. The HPL of the ansatz are functions of $\rho = \sqrt{\zeta}$, and their natural local variable at the endpoint is $1-\rho$ rather than $y = (1-\rho)(1+\rho)$. If we re-expand in y, their endpoint values contain powers of $\log 2$ at every weight, whereas the Sudakov series contains none. The cancellation of all $\log 2$ terms at order y^0 is therefore a set of equations in its own right, separate from matching the $\log 2$-free coefficients. The elliptic iterated integrals obey a stronger version of the same requirement: their values at the cusp $\zeta = 1$ involve periods of level six outside the multiple zeta values, such as the sixth-root-of-unity constant in $S_0(1)$ of Eq. (73), and these must cancel at order y^0 as well. Using this needs the expansion of each elliptic iterated integral at the second cusp.

(C4) Higher powers. At next-to-leading power in the back-to-back limit, order y^0 in $d\sigma/d\zeta$ and order y^1 in F, the two highest logarithms are known from the subleading-power resummation [18, 78]: at NNLO the coefficients $\frac{1}{10}$ and $-\frac{1}{3}$ of $y\log^5 y$ and $y\log^4 y$ in Eq. (73). In principle, further powers in either expansion can be obtained from expanding the integrand and integrating. But they are computations rather than physical constraints.

(C5) Sum rules. EEC satisfies two sum rules:

$$\int_0^1 d\zeta \frac{d\sigma}{d\zeta} = \sigma_{\text{tot}}, \qquad \int_0^1 d\zeta\,\zeta \frac{d\sigma}{d\zeta} = \frac{1}{2}\sigma_{\text{tot}}\,. \tag{85}$$

Here σ_{tot} is the total cross-section in a given process. Note that in the sum rule, one has to also include the contact terms $\delta(\zeta)$ and $\delta(1-\zeta)$. These terms are considered as the singular terms, similar to the large logs $\log(\zeta)$ and $\log(1-\zeta)$. Therefore, they can be predicted from light-ray OPE in $\mathcal{N}=4$ SYM, and from effective field theories in QCD.

At NLO we will impose the zeroth sum rule channel by channel (Table I), while at NNLO we will impose neither. The moments of the complete elliptic sector are multiple zeta values, as the sum rule requires. However, the integrals of individual elliptic basis elements are not. To properly impose the sum rule, we will need to work out these integrals analytically. We skip this because it does not buy us many constraints.

The above physical constraints cannot determine the unknown parameters of the bootstrap: 130 of 206 parameters remain undetermined at NLO and 1963 of 2336 at NNLO. This is precisely why bootstrapping cross-section observables or QCD amplitudes is difficult. Unlike planar $\mathcal{N}=4$

SYM amplitudes or form factors, we need to determine the rational coefficients, and each function is expressed with many unknown parameters. The number of physical constraints is far from enough. As proposed in Ref. [55], one can equip a bootstrap program with analytic regression from high-precision numerical data. There are different approaches to perform the analytic regression. The most straightforward method is the linear fit, where one obtains floating-point numbers for all unknown parameters. These values can then be reconstructed as rational numbers and transcendental numbers like π and ζ_n through PSLQ. Alternatively, as introduced in Ref. [55], one can use lattice reduction to search for integer relations among the function itself and all the transcendental basis. Lattice reduction can use either one or multiple numerical points, where one numerical point is the same as PSLQ.

In general, a bootstrap program equipped with analytic regression requires a numerical routine to calculate the observables or amplitudes to high precision. We do not have one for NNLO EEC. However, as a first look, we can generate fake numerical data from the analytic expression and test how robust the bootstrap method can be. The exercises in the next subsection will follow this spirit.

D. Results

With the function space of Sec. V A, the coefficient ansatz of Sec. V B and the conditions of Sec. V C in hand, we carry out the bootstrap at the three known orders. Throughout, the HPLs have argument $\rho = \sqrt{\zeta}$, suppressed as in Sec. IV C. LO and NLO are purely polylogarithmic; NNLO includes the elliptic sector. We will report the number of unknown parameters along the procedure.

1. LO and NLO bootstrap

The LO EEC is simple enough to bootstrap without any numerical data input. We first work with the two rational letters and then admit the third letter. With $H_0 = \log\zeta$ and $H_1 = -\log(1-\zeta)$ the ansatz is $p_0(\zeta)+p_1(\zeta)H_0+p_2(\zeta)H_1$ with quadratic polynomials p_i and the number of unknown parameters is nine. The logarithm bound of (C1) removes the three coefficients of p_1; the collinear condition $F_{\rm LO} = \zeta + \mathcal{O}(\zeta^2)$ gives two equations; the back-to-back condition $F_{\rm LO} \to -\log y$ gives two; the two sum rules give four, of which two are independent of the rest. The chain is $9 \to 6 \to$

$4 \to 2 \to 0$, and the unique solution is

$$F_{\rm LO}(\zeta) = -\log(1-\zeta) = H_- \,, \tag{86}$$

in the notation of Eq. (66). If we include the square-root letter of Eq. (78), two further terms, odd in $\sqrt{\zeta}$, enter the ansatz and the number of unknown parameters becomes eleven. The same conditions give the same answer, with the two new coefficients zero.

It is worth emphasizing that the numerator degree of freedom d in Eq. (83) is unknown beforehand and may differ among coefficients. One picks a d, runs the program, and raises d if the conditions are inconsistent; once a d works, raising it further tests the stability of the result. For LO EEC, $d = 2$ already closes the system from the physical constraints alone. We then verify that $d = 3$ also gives the same answer.

At NLO the total weight is at most three, so the basis is the 40 HPLs of weight zero to three carrying the constants 1, π^2 and ζ_3, adding up to 45 basis functions (26 even and 19 odd). With $m_0 = m_1 = 1$ and $d = 4$, each even basis function carries five numerator coefficients and each odd one four, so Eq. (83) has 206 unknown rational parameters. Tab. I summarizes the number of parameters after applying each constraint. Regularity alone removes 43, the leading-power data at the two endpoints remove 22 more, and the zeroth sum rule removes 11. In all, 76 of the 206 parameters are fixed without sampled values.

The remaining 130 parameters can be fixed from sampled values. As mentioned above, we are doing this study to test the ability of the bootstrap, so we use the numerical evaluation of the true answer to some precision as data. In a realistic bootstrap program, one needs to have an independent numerical evaluator of the observable. We sample 126 points to around 180 digits and use a linear solver to determine the unknown parameters. The resulting floating-point numbers are then rationalized to get the analytic form. If the sum rule is not applied, then we need 134 points at 200 digits. We also perform two further consistency checks: (1) raise the powers of the denominator to $m_0 = m_1 = 2$ or 3, while keeping $d = 2 + m_0 + m_1$; (2) raise the numerator degree to $d = 5$ or 6, with $m_0 = m_1 = 1$ fixed. In both cases, we find the same final answer and thus verify the stability of this procedure.

We also run the lattice reduction for the final steps. We test the performance with different numbers of points and various precision digits. The number of digits required decreases with the number of sample points and saturates at 25. The comparison with linear solve is given in Tab. II.

At the end we find the following NLO expression $F_{\rm NLO} = F^{[2]} + F^{[3]}$, with

$$F^{[2]} = (\zeta-1)\left[4H_{-,0} - 4\sqrt{\zeta}H_{+,0} - 4\zeta H_{0,-} - 2\,(\zeta-1)\,H_{-,-} - \frac{\pi^2}{3}\zeta\right] , \tag{87}$$

NLO, 206 parameters	equations	left
ansatz: weights 0–3, $m_0 = m_1 = 1$, $d = 4$, parity in ρ	—	206
no power divergence at $\zeta = 0$	7	199
nothing at order ζ^0	7	192
no power divergence at $\zeta = 1$	14	178
at most $\log \zeta$ at every order in ζ	15	163
at most $\log^3 y$; integer local exponents	0	163
regularity, subtotal	43	163
collinear ζ^1 bracket, light-ray OPE	5	158
back-to-back y^0 bracket, Sudakov, $\log 2$-free	7	151
the $\log 2$ structures must cancel	7	144
y^1 coefficients of $\log^3 y$ and $\log^2 y$	3	141
all analytic conditions, subtotal	65	141
the zeroth sum rule	11	130
linear solve, 126 points at 180 digits	—	0

TABLE I. The NLO EEC bootstrap on the 206-parameter ansatz. The number of equations and the unknown parameters at each step are listed. Finally, the remaining 130 parameters can be determined by numerical data.

sample points N	lattice reduction	linear solve
8	50–52	—
16	30–32	—
32	26–28	—
48	25–26	—
126	25	174–188
260	25	160

TABLE II. Precision digits needed to determine the remaining parameters in the NLO EEC bootstrap, using both lattice reduction and linear solve. After having enough sampling points, the required precision saturates at 25 digits.

and

$$\begin{aligned} F^{[3]} = {} & 4\zeta\,(\zeta-2)\,H_{0,0,-} - 2\zeta\,(4\zeta-3)\,H_{0,-,0} - \zeta\,(2\zeta+1)\,H_{0,-,-} \\ & + \left(2\zeta^2-3\zeta-4\right) H_{-,0,-} - \zeta\,(4\zeta-3)\,H_{-,-,0} - \left(\zeta^2+2\right) H_{-,-,-} \\ & + (\zeta-1)\,(2\zeta+1)\,H_{+,+,0} + \frac{\pi^2\zeta^2}{3} H_0 + \frac{\pi^2}{12}\left(2\zeta^2+\zeta-2\right) H_- - \frac{\zeta\,(4\zeta+1)}{2}\zeta_3\,, \end{aligned} \tag{88}$$

which agrees term by term with Ref. [6]. Exactly one odd harmonic polylogarithm survives, $H_{+,0}$, with its compulsory factor $\sqrt{\zeta}$.

2. NNLO bootstrap

At NNLO both sectors are present and every condition applies to their sum, so the two ansätze are added before anything is imposed. In the polylogarithmic sector the basis of total weight at most five has 423 elements, 220 even and 203 odd; with $m_0 = m_1 = 0$ and $d = 2$, the pole-free form, since neither the collinear nor the back-to-back limit allows a power divergence, this gives 1066 unknown parameters. In the elliptic sector, we do not use the restriction of the kernels to $\mathcal{A}^{(3)}$ or of the tails to ω_0, ω_1 as input but let the bootstrap decide. With all four kernels $\psi_1^3\{1, \zeta, \zeta^2, \zeta^3\}$ of M_3 and all three letters of M_2 as tails, Eq. (82) has 124 iterated integrals plus the three homogeneous terms. Each has the two prefactors of Eq. (84) of five coefficients, which leads to 1270 unknown parameters. In total, we have 2336 parameters to be determined.

NNLO, joint, 2336 parameters	equations	left
polylogarithmic ansatz, weights 0–5, $m_0 = m_1 = 0$, $d = 2$	—	1066
elliptic ansatz, all 127 words, prefactors free, degree ≤ 4	—	1270
no power divergence at $\zeta = 0$, nothing at order ζ^0	21	2315
no power divergence at $\zeta = 1$	59	2256
at most $\log^2 \zeta$ at every order in ζ	81	2175
at most $\log^5 y$; integer local exponents	0	2175
collinear ζ^1 bracket, light-ray OPE	13	2162
back-to-back y^0 bracket, Sudakov, $\log 2$-free; the $\log 2$ structures cancel	199	1963
reorganization	113	1850
lattice reduction:		
# of points = 150, digit = 350, time = 119.5 cpu hours		
# of points = 300, digit = 270, time = 50.4 cpu hours		
# of points = 600, digit = 225, time = 56.1 cpu hours		
# of points = 1200, digit = 205, time = 62.1 cpu hours		

TABLE III. The NNLO bootstrap on the joint ansatz. The number of parameters left after each constraint is listed. In the reorganization step, some unknowns appear only in specific linear combinations, which we replace with new variables. The physical constraints leave 1963 of 2336 parameters and the reorganization 1850. We perform four lattice-reduction setups to regress the 1850 parameters, as shown in the last block. The CPU hours are recorded on a machine with an Intel Xeon Platinum 8581C (2.30 GHz, 48 cores, 96 hardware threads), using 32 threads and up to 21 GB of memory.

Tab. III lists the number of parameters after each constraint. Regularity removes 161 and the leading-power data in the two limits 212, in all 373 of 2336. Compared to NLO, only 16%

of the parameters are determined by the physical constraints. The next-to-leading back-to-back logarithms of (C4) are not needed: the reduction below closes without them. After that, it turns out that some of the parameters only appear in certain linear combinations, so we can define new parameters to replace these combinations. This further reduces 113 parameters, and we are left with 1850 unknowns.

We again test the lattice reduction on the remaining parameters with fake numerical data generated from the analytic expression. We use FLATTER [79] to perform the reduction. As shown in the last block of Table III, with 150 numerical points and 350 digits we can determine the remaining 1850 parameters all at once, and more points buy fewer digits per point: 300 points at 270 digits, 600 at 225, and 1200 at 205 also return the exact coefficient vector. An information count of the sample set (the lattice volume above 10^{-P} for N points at P digits) indicates that this gain levels off near 200 digits per point, and that at 100 digits or fewer no number of points up to 2400 suffices.

The lesson we learn from the NNLO bootstrap is that physical constraints are far from complete to determine an expression with rational coefficients. In this example, 80% of parameters are fixed from the numerical data. On the one hand, this suggests that we need to explore the analytic structure of energy correlators and come up with more consistency conditions. One direction is to cleanly separate the polylogarithmic sector from the elliptic sector. The NNLO EEC in $\mathcal{N}=4$ SYM is computed from the four-point correlator, which makes the separation challenging. It will be interesting to see if the Integration-by-Parts [80–82] and differential equations [83–86] approach provides a handle for identifying elliptic sectors. On the other hand, the analytic regression with numerical data is powerful enough to accurately reconstruct the analytic result. This implies that numerical data contains more hidden information and it is important to develop numerical frameworks for precise evaluation.

VI. CONCLUSIONS

In this paper, we have completed the analytic calculation of the energy–energy correlator in $\mathcal{N}=4$ SYM at NNLO. The result of Ref. [1] consists of HPLs up to weight five, together with one two-fold integral over a polylogarithmic integrand, which had resisted evaluation. A partial fraction guided by the Galois symmetry of the square root in that integrand separates it into a piece that integrates to HPLs and two irreducible pieces that live on a single elliptic curve. This curve is the curve of the equal-mass sunrise integral: the two j-invariants agree identically under a Möbius

map, so that the elliptic sector of the EEC is built from the modular forms of $\Gamma_1(6)$. Solving the associated Picard–Fuchs system reduces the elliptic part of the correlator to a single function S_0 and its first derivative, multiplied by two rational functions. S_0 itself is the period ψ_1 times a finite combination of iterated Eisenstein integrals whose coefficients are rational multiples of 1, π^2, ζ_3, π^4, ζ_5 and $\pi^2\zeta_3$, Eq. (61). The complete result, $F_{\mathrm{NNLO}} = F_{\mathrm{P}} + F_{\mathrm{E}}$, is given in Sec. IV C. Since the iterated Eisenstein integrals are q-series with rational coefficients, the elliptic sector can be evaluated to high precision as readily as the polylogarithmic one. We also provide the expansions of the NNLO correlator to subleading powers in both the collinear and the back-to-back limits.

The closed form makes possible a first look at a perturbative bootstrap of the EEC. At LO, at NLO and in the polylogarithmic sector at NNLO, the function space is standard, spanned by HPLs in the three letters ζ, $1-\zeta$ and $(1-\sqrt{\zeta})/(1+\sqrt{\zeta})$. In the elliptic sector, the curve, the Picard-Fuchs operator and the location of the physical singularities restrict the kernels to six, which allows us to write down an elliptic ansatz. That the resulting function space is finite is far from automatic, and it indicates how bootstrap methods may be extended to observables with elliptic sectors. We further formulate a general ansatz for the rational coefficients and collect the physical constraints that the observable supplies. Then we show that the parameters these leave undetermined can be fixed from numerical data by analytic regression, in particular by lattice reduction. In this first study, the data for these tests were generated from the analytic result of this paper rather than from an independent numerical evaluator of the EEC.

Both the direct calculation and the bootstrap study carry lessons for QCD. The elliptic function space is fixed by geometry rather than by the details of the theory. The curve and its level follow from the maximal cut of the integrand, and thus it will be interesting to perform the corresponding analysis for the QCD integrand. Once the curve and level are known, the elliptic letters and the function space follow as they did here. A complete bootstrap of the NNLO correlator in QCD remains difficult, but knowing the function space in advance can bypass intermediate steps of a direct calculation and simplify its result. Finally, the q-series evaluation of iterated Eisenstein integrals used here will also allow the QCD result, once obtained, to be evaluated quickly and to high precision, which will be crucial for phenomenological studies at colliders. With the elliptic sector of the simplest event shape now under the same control as its polylogarithmic part, both analytically and numerically, the way is open to bring the same tools to bear on precision QCD.

ACKNOWLEDGMENTS

Funding for this project was provided by Anthropic. This is not an official Anthropic project and results and views are not endorsed by Anthropic. XYZ is supported by the MIT Pappalardo Fellowship.

Appendix A: Function classes and conventions

Generalized polylogarithms. The generalized polylogarithm is defined as [87]

$$G(a_1,\dots,a_n;x)=\int_0^x \frac{dt}{t-a_1}\,G(a_2,\dots,a_n;t)\,,\qquad G(\,;x)=1\,, \tag{A1}$$

with a_1 outermost; the length n is the transcendental weight. For $a_n=0$ the innermost integration diverges and we use the standard regularization

$$G(0^{\,k};x)=\frac{\log^k x}{k!}\,,\qquad G(a_1,\dots,a_m;x)\,G(a_{m+1},\dots,a_{m+n};x)=\sum_{\sigma} G\big(a_{\sigma(1)},\dots,a_{\sigma(m+n)};x\big)\,, \tag{A2}$$

the sum running over the interleavings that preserve the order within each factor (the shuffle product), which expresses every G with trailing zeros through convergent ones, e.g. $\log x\,G(0,1;x)=2G(0,0,1;x)+G(0,1,0;x)$. Appendix B lists its functions in the form

$$f(\zeta)=\sum_{w}\kappa_w(\zeta)\,G(w;\zeta)\,, \tag{A3}$$

with w running over index vectors with entries in $\{0,1\}$, including the empty one, and κ_w rational functions of ζ times constants from $\{1,\pi^2,\zeta_3,\pi^4,\zeta_5,\pi^2\zeta_3\}$; the weight of a term is the length of w plus the weight of its constant. Numerically we evaluate the G's with Refs. [35, 73].

Harmonic polylogarithms [66] are the case $a_i\in\{0,1\}$ with the kernel of the index 1 taken as $1/(1-t)$, so that

$$H_u(\zeta)=(-1)^{\,n_1(u)}\,G(u;\zeta)\,, \tag{A4}$$

$n_1(u)$ being the number of 1's in u; thus $H_0=\log\zeta$, $H_1=-\log(1-\zeta)$ and $H_{0^{\,n-1},1}=\mathrm{Li}_n$. Two subscript conventions occur in the text. In the expanded notation (Sec. IV B, Eq. (48)) the subscript is the full index vector. In the condensed notation of Ref. [66] (Eq. (43)) an index $m\geq 1$ stands for $m-1$ zeros followed by a 1, e.g. $H_4=H_{0,0,0,1}$, $H_{3,0}=H_{0,0,1,0}$, $H_{1,2}=H_{1,0,1}$; the sign in (A4) is always read off the expanded form. The letters $\pm$ for arguments $\sqrt{\zeta}$ are defined in Eq. (66). Both conventions are implemented in Ref. [72].

Iterated Eisenstein integrals. In the frame of Eq. (49), with $L = \log q$ and $\theta = q\,d/dq$, the iterated integrals of Sec. IV B are $I(f_1,\ldots,f_n;q) = \theta^{-1}[f_1\,I(f_2,\ldots,f_n;q)]$ with $I(\,;q) = 1$, f_1 outermost, the length again being the transcendental weight; θ^{-1} acts on $\mathbb{Q}[[q]][L]$ by the rules of Eq. (58), which correspond to the tangential base point at $q = 0$, introduce no integration constants, and preserve the shuffle product. "Weight" thus has two senses, the transcendental weight of an iterated integral and the modular weight of a letter. Harmonic polylogarithms of ζ are the special case in which every letter has modular weight two: since $\theta \log\zeta = \omega_0$ and $\theta[-\log(1-\zeta)] = \omega_1$, one has $\log\zeta = I(\omega_0;q)$ and $H_u(\zeta) = I(\omega_{u_1},\ldots,\omega_{u_n};q)$ for u ending in 1, so the polylogarithmic sector lies in the same function class as the elliptic one. Whether a given q-series is an admissible letter of modular weight k is decided by the criterion below Eq. (53); the four letters of Eq. (54) were identified in this way.

Both classes are standard: multiple polylogarithms [66, 87], in which two-fold integrals such as Eq. (17) can be done directly when linearly reducible [69, 88], and iterated integrals of modular forms for $\Gamma_1(6)$, the class of the equal-mass sunrise [58]. After the inner integration over x of the two-fold representation, Eq. (34), is done in closed form, the outer integrand is an elliptic multiple polylogarithm in the sense of Ref. [61], its algebraic letters being the roots of $D_1(x)$, which carry $\sqrt{Q_1(\bar{z})}$ of Eq. (20); the integrated result, Eq. (61), nevertheless requires only the smaller class.

Appendix B: The sources of the elliptic system

In this appendix, we provide the analytic expressions for E and E', the sources of the elliptic system defined by Eq. (44). Both sources are at most weight four. Explicitly, we have

$$\begin{aligned}
E(\zeta) = &-\frac{64\zeta^2+3\zeta-1}{2\zeta} - \frac{3\,(4\zeta-3)\,(4\zeta+1)}{4\zeta}\,G(1;\zeta) - \frac{(2\zeta+1)^2}{\zeta}\,G(0;\zeta) + \frac{(\zeta-1)\,(\zeta+2)}{\zeta}\,G(1,1;\zeta)\\
&- \frac{18\zeta^3-31\zeta^2-16\zeta-1}{2\zeta\,(\zeta-1)}\,G(0,1;\zeta) + \frac{6\zeta^2-\zeta+1}{2\zeta}\,G(1,0;\zeta) + (5\zeta+1)\;G(0,0;\zeta)\\
&+ \frac{4\zeta^3+66\zeta^2-3\zeta-7}{24\zeta\,(\zeta-1)}\,\pi^2 + \frac{2\zeta^2+1}{\zeta}\Big[G(0,1,0;\zeta) - G(1,0,0;\zeta)\Big]\\
&- \frac{24\zeta^4-288\zeta^3+208\zeta^2+19\zeta-8}{4\zeta\,(\zeta-1)}\,\zeta_3 - \frac{2\,(\zeta-1)\,\big(3\zeta^2-1\big)}{\zeta}\,G(0,1,1;\zeta)\\
&- \frac{(2\zeta+1)\,\big(12\zeta^3-54\zeta^2+35\zeta-8\big)}{4\zeta\,(\zeta-1)}\,G(1,0,1;\zeta) + \frac{24\zeta^3-88\zeta^2+8\zeta+11}{4\,(\zeta-1)}\,G(0,0,1;\zeta)\\
&+ \frac{2\,(\zeta-1)^2\,(3\zeta+2)}{\zeta}\,G(1,1,1;\zeta) + \frac{40\zeta^3+8\zeta^2+5\zeta-8}{24\zeta\,(\zeta-1)}\,\pi^2\,G(1;\zeta)\\
&- \frac{(4\zeta-1)\,(4\zeta+1)}{12\zeta}\,\pi^2\,G(0;\zeta) + \frac{2\zeta+1}{60}\,\mathcal{W}_1\,,
\end{aligned} \tag{B1}$$

and

$$
\begin{aligned}
E'(\zeta) = &-\frac{1}{2\zeta}\Big[24 + 24\,G(1;\zeta) - 6\,G(0,0;\zeta) + 6\,G(1,0;\zeta) + 9\,G(0,1,0;\zeta) - 9\,G(1,0,0;\zeta) \\
&+ 2\,\pi^2\,G(0;\zeta)\Big] - \frac{12\,(\zeta-1)}{\zeta}\,G(1,1;\zeta) + \frac{6\left(2\zeta^2-4\zeta+1\right)}{\zeta\,(\zeta-1)}\,G(0,1;\zeta) - \frac{2\zeta^2+\zeta-2}{\zeta\,(\zeta-1)}\,\pi^2 \\
&- \frac{28\zeta^2-81\zeta+62}{2\zeta\,(\zeta-1)}\,\zeta_3 - \frac{28\zeta-23}{2\zeta}\,G(0,1,1;\zeta) - \frac{28\zeta^2-41\zeta+22}{2\zeta\,(\zeta-1)}\,G(1,0,1;\zeta) \\
&+ \frac{28\zeta^2-18\zeta-1}{2\zeta\,(\zeta-1)}\,G(0,0,1;\zeta) + \frac{14\zeta-23}{\zeta}\,G(1,1,1;\zeta) - \frac{11\zeta-8}{4\zeta\,(\zeta-1)}\,\pi^2\,G(1;\zeta) - \frac{4\zeta-1}{60\zeta}\,\mathcal{W}_1\,,
\end{aligned}
\tag{B2}
$$

where both $E(\zeta)$ and $E'(\zeta)$ contain

$$
\begin{aligned}
\mathcal{W}_1 \;=\; &120\,G(0,0,0,1;\zeta) + 60\,G(0,0,1,1;\zeta) - 60\,G(0,1,0,1;\zeta) \\
&- 120\,G(0,1,1,1;\zeta) - 240\,G(1,0,0,1;\zeta) + 60\,G(1,0,1,1;\zeta) + 180\,G(1,1,0,1;\zeta) \\
&- 15\,\pi^2\,G(0,0;\zeta) - 30\,\pi^2\,G(0,1;\zeta) + 15\,\pi^2\,G(1,0;\zeta) + 30\,\pi^2\,G(1,1;\zeta) \\
&+ 420\,\zeta_3\,G(0;\zeta) - 300\,\zeta_3\,G(1;\zeta) - 4\,\pi^4\,.
\end{aligned}
\tag{B3}
$$

The weight-four bracket drops out of the combination that drives Eq. (56): by Eq. (A4) the last brace of Eq. (48) equals $-\mathcal{W}_1/90$, so $\beta'\Psi$ contains $+\frac{4\zeta-1}{60\zeta}\,\mathcal{W}_1$, which cancels the last term of Eq. (B2); the source $E'+\beta'\Psi$ is therefore of weight at most three, as used in Sec. V A. The sources of the second channel, which enter Eq. (44) in the same way, are

$$
\begin{aligned}
E_{R_2}(\zeta) = &\frac{\zeta\,(2\zeta-1)\,(8\zeta+1)}{\zeta-1} + \frac{32\zeta^3-46\zeta^2-12\zeta-1}{2\,(\zeta-1)}\,G(1;\zeta) + \frac{\zeta\left(16\zeta^2-23\zeta-2\right)}{\zeta-1}\,G(0;\zeta) \\
&- \frac{11\zeta^2-2\zeta+6}{\zeta-1}\,G(1,0;\zeta) - \frac{96\zeta^4-134\zeta^3+78\zeta^2-9\zeta-1}{2\,(\zeta-1)^2}\,G(0,1;\zeta) \\
&+ \left(24\zeta^2-11\zeta+2\right)\,G(1,1;\zeta) - \frac{\zeta\left(24\zeta^2-11\zeta+2\right)}{\zeta-1}\,G(0,0;\zeta) - \frac{\zeta\left(24\zeta^3+7\zeta^2-14\zeta-2\right)}{6\,(\zeta-1)^2}\,\pi^2 \\
&+ \frac{3\zeta\left(12\zeta^3-36\zeta^2+24\zeta+13\right)}{2\,(\zeta-1)^2}\,\zeta_3 + \frac{28\zeta^2+3\zeta-7}{2\,(\zeta-1)}\,G(1,0,0;\zeta) \\
&+ \frac{4\zeta^3-3\zeta^2+62\zeta+3}{2\,(\zeta-1)^2}\,G(0,1,0;\zeta) - \frac{36\zeta^4-160\zeta^3+157\zeta^2+\zeta+5}{2\,(\zeta-1)^2}\,G(0,0,1;\zeta) \\
&+ \frac{18\zeta^3-64\zeta^2+30\zeta-5}{\zeta-1}\,G(0,1,1;\zeta) + \frac{36\zeta^4-84\zeta^3+97\zeta^2+27\zeta+29}{2\,(\zeta-1)^2}\,G(1,0,1;\zeta) \\
&- 6\left(3\zeta^2-4\zeta+2\right)\,G(1,1,1;\zeta) - \frac{36\zeta^3-70\zeta^2-69\zeta-2}{12\,(\zeta-1)^2}\,\pi^2\,G(1;\zeta) + \frac{\zeta\left(32\zeta^2+1\right)}{6\,(\zeta-1)^2}\,\pi^2\,G(0;\zeta) \\
&- \frac{36\zeta^3-5\zeta^2-40\zeta+3}{2\,(\zeta-1)^2}\Big[G(1,0,0,1;\zeta) - \zeta_3\,G(1;\zeta)\Big] \\
&+ \frac{148\zeta^3-168\zeta^2-9\zeta-1}{12\,(\zeta-1)^2}\Big[6\,G(1,1,0,1;\zeta) + \pi^2\,G(1,1;\zeta)\Big]
\end{aligned}
$$

$$
\begin{aligned}
&+\frac{\zeta\left(160\zeta^2-173\zeta-45\right)}{80\left(\zeta-1\right)^2}\,\pi^4-\frac{3\zeta\left(10\zeta^2-14\zeta-3\right)}{\left(\zeta-1\right)^2}\,\zeta_3\,G(0;\zeta)\\
&-\frac{32\zeta^3-40\zeta^2+25\zeta+1}{2\left(\zeta-1\right)^2}\,G(0,1,0,0;\zeta)-\frac{\zeta\left(90\zeta^2-92\zeta-25\right)}{\left(\zeta-1\right)^2}\,G(0,0,1,0;\zeta)\\
&+\frac{84\zeta^3-112\zeta^2+7\zeta-3}{2\left(\zeta-1\right)^2}\,G(1,0,1,0;\zeta)+\frac{92\zeta^3-158\zeta^2+5\zeta+1}{2\left(\zeta-1\right)^2}\,G(0,0,0,1;\zeta)\\
&-\frac{182\zeta^3-228\zeta^2+15\zeta+1}{\left(\zeta-1\right)^2}\,G(0,1,0,1;\zeta)-\frac{\zeta\left(30\zeta^2-71\zeta+23\right)}{\left(\zeta-1\right)^2}\,G(0,0,1,1;\zeta)\\
&-\frac{28\zeta^2-23\zeta+1}{2\left(\zeta-1\right)}\,G(1,0,1,1;\zeta)+\frac{12\zeta\left(5\zeta-4\right)}{\zeta-1}\,G(0,1,1,1;\zeta)\\
&-\frac{\zeta\left(60\zeta^2-67\zeta-17\right)}{4\left(\zeta-1\right)^2}\,\pi^2\,G(0,1;\zeta)+\frac{\zeta\left(41\zeta-65\right)}{12\left(\zeta-1\right)^2}\,\pi^2\,G(1,0;\zeta)-\frac{\zeta\left(17\zeta+1\right)}{12\left(\zeta-1\right)^2}\,\pi^2\,G(0,0;\zeta)\\
&-\frac{32\zeta^3-24\zeta^2-3\zeta+1}{240\left(\zeta-1\right)^2}\,\mathcal{W}_2\,,
\end{aligned}
\tag{B4}
$$

and

$$
\begin{aligned}
E'_{R_2}(\zeta)=&\frac{2\zeta^2-2\zeta+1}{\left(\zeta-1\right)^2}\Big[6\,G(0,1;\zeta)+\pi^2\Big]-\frac{6\left(2\zeta^2-4\zeta+1\right)}{\zeta\left(\zeta-1\right)}\,G(1,0;\zeta)-\frac{6\left(2\zeta-1\right)}{\zeta}\,G(1,1;\zeta)\\
&+\frac{6\left(2\zeta-1\right)}{\zeta-1}\,G(0,0;\zeta)+\frac{1}{40\left(\zeta-1\right)^2}\,\mathcal{W}_2-\frac{1}{\left(\zeta-1\right)^2}\,\pi^2\,G(0;\zeta)\\
&-\frac{28\zeta^3-49\zeta^2+14\zeta+1}{2\zeta\left(\zeta-1\right)^2}\,\zeta_3\\
&+\frac{5\zeta^2-6\zeta-1}{4\zeta\left(\zeta-1\right)^2}\,\pi^2\,G(1;\zeta)+\frac{3\left(3\zeta-5\right)}{2\zeta\left(\zeta-1\right)}\,G(1,0,0;\zeta)+\frac{3\left(5\zeta^2-8\zeta-1\right)}{2\zeta\left(\zeta-1\right)^2}\,G(0,1,0;\zeta)\\
&+\frac{\left(2\zeta-1\right)\left(7\zeta^2-11\zeta+1\right)}{\zeta\left(\zeta-1\right)^2}\,G(0,0,1;\zeta)-\frac{\left(4\zeta-5\right)\left(7\zeta-1\right)}{2\zeta\left(\zeta-1\right)}\,G(0,1,1;\zeta)\\
&-\frac{28\zeta^3-105\zeta^2+126\zeta-43}{2\zeta\left(\zeta-1\right)^2}\,G(1,0,1;\zeta)+\frac{14\zeta-17}{\zeta}\,G(1,1,1;\zeta)\\
&-\frac{4\zeta^3-9\zeta^2-1}{30\zeta\left(\zeta-1\right)^2}\Big[90\,G(0,0,1,0;\zeta)+15\,\pi^2\,G(0,1;\zeta)+30\,\zeta_3\,G(0;\zeta)-2\,\pi^4\Big]\\
&+\frac{4\zeta^3-9\zeta^2+9\zeta+2}{\zeta\left(\zeta-1\right)^2}\Big[G(1,0,0,1;\zeta)-\zeta_3\,G(1;\zeta)\Big]\\
&+\frac{4\zeta^2-9\zeta+1}{2\left(\zeta-1\right)^2}\Big[6\,G(1,1,0,1;\zeta)+\pi^2\,G(1,1;\zeta)\Big]\\
&-\frac{4\zeta^2-5\zeta-5}{\zeta\left(\zeta-1\right)}\Big[G(0,0,1,1;\zeta)-2\,G(0,1,1,1;\zeta)\Big]-\frac{1}{\zeta\left(\zeta-1\right)^2}\,\pi^2\,G(1,0;\zeta)\\
&+\frac{3}{\zeta\left(\zeta-1\right)}\,G(0,1,0,0;\zeta)+\frac{3\left(4\zeta^2-9\zeta+3\right)}{\left(\zeta-1\right)^2}\,G(1,0,1,0;\zeta)\\
&+\frac{4\zeta^3-9\zeta^2-3\zeta+2}{\zeta\left(\zeta-1\right)^2}\,G(0,0,0,1;\zeta)-\frac{20\zeta^3-45\zeta^2-6\zeta+7}{\zeta\left(\zeta-1\right)^2}\,G(0,1,0,1;\zeta)\\
&-\frac{4\zeta^2-5\zeta-2}{\zeta\left(\zeta-1\right)}\,G(1,0,1,1;\zeta)\,.
\end{aligned}
\tag{B5}
$$

where both $E_{R_2}(\zeta)$ and $E'_{R_2}(\zeta)$ contain the weight-five bracket

$$\begin{aligned}\mathcal{W}_2 \;=\;& 360\,G(0,0,0,1,0;\zeta) - 240\,G(0,0,0,1,1;\zeta) - 120\,G(0,0,1,0,0;\zeta) + 480\,G(0,0,1,1,1;\zeta)\\ &+ 240\,G(0,1,0,0,1;\zeta) - 120\,G(0,1,0,1,1;\zeta) - 120\,G(0,1,1,0,1;\zeta) + 480\,G(1,0,0,0,1;\zeta)\\ &- 600\,G(1,0,0,1,0;\zeta) - 240\,G(1,0,0,1,1;\zeta) + 120\,G(1,0,1,0,0;\zeta) - 720\,G(1,0,1,0,1;\zeta)\\ &- 120\,G(1,1,0,0,1;\zeta) + 240\,G(1,1,0,1,0;\zeta) + 360\,G(1,1,1,0,1;\zeta)\\ &+ 60\,\pi^2\,G(0,0,1;\zeta) - 60\,\pi^2\,G(0,1,0;\zeta) - 20\,\pi^2\,G(0,1,1;\zeta) + 20\,\pi^2\,G(1,0,0;\zeta)\\ &- 120\,\pi^2\,G(1,0,1;\zeta) + 40\,\pi^2\,G(1,1,0;\zeta) + 60\,\pi^2\,G(1,1,1;\zeta)\\ &+ 120\,\zeta_3\,G(0,0;\zeta) - 240\,\zeta_3\,G(0,1;\zeta) - 360\,\zeta_3\,G(1,0;\zeta) + 120\,\zeta_3\,G(1,1;\zeta)\\ &- 8\,\pi^4\,G(0;\zeta) + 15\,\pi^4\,G(1;\zeta) + 1980\,\zeta_5 - 20\,\pi^2\zeta_3\,. \end{aligned} \tag{B6}$$

[1] J. M. Henn, E. Sokatchev, K. Yan, and A. Zhiboedov, Phys. Rev. D **100**, 036010 (2019), arXiv:1903.05314 [hep-th].

[2] C. L. Basham, L. S. Brown, S. D. Ellis, and S. T. Love, Phys. Rev. Lett. **41**, 1585 (1978).

[3] C. L. Basham, L. S. Brown, S. D. Ellis, and S. T. Love, Phys. Rev. D **19**, 2018 (1979).

[4] C. L. Basham, L. S. Brown, S. D. Ellis, and S. T. Love, Phys. Lett. B **85**, 297 (1979).

[5] C. L. Basham, L. S. Brown, S. D. Ellis, and S. T. Love, Phys. Rev. D **17**, 2298 (1978).

[6] A. V. Belitsky, S. Hohenegger, G. P. Korchemsky, E. Sokatchev, and A. Zhiboedov, Phys. Rev. Lett. **112**, 071601 (2014), arXiv:1311.6800 [hep-th].

[7] L. J. Dixon, M.-X. Luo, V. Shtabovenko, T.-Z. Yang, and H. X. Zhu, Phys. Rev. Lett. **120**, 102001 (2018), arXiv:1801.03219 [hep-ph].

[8] M.-X. Luo, V. Shtabovenko, T.-Z. Yang, and H. X. Zhu, JHEP **06**, 037 (2019), arXiv:1903.07277 [hep-ph].

[9] J. Gao, V. Shtabovenko, and T.-Z. Yang, JHEP **02**, 210 (2021), arXiv:2012.14188 [hep-ph].

[10] L. J. Dixon, I. Moult, and H. X. Zhu, Phys. Rev. D **100**, 014009 (2019), arXiv:1905.01310 [hep-ph].

[11] M. Kologlu, P. Kravchuk, D. Simmons-Duffin, and A. Zhiboedov, JHEP **01**, 128 (2021), arXiv:1905.01311 [hep-th].

[12] G. P. Korchemsky, JHEP **01**, 008 (2020), arXiv:1905.01444 [hep-th].

[13] J. C. Collins and D. E. Soper, Nuclear Physics B **193**, 381 (1981).

[14] S. Ellis, D. Richards, and W. Stirling, Physics Letters B **136**, 99 (1984).

[15] D. de Florian and M. Grazzini, Nucl. Phys. B **704**, 387 (2005), arXiv:hep-ph/0407241.

[16] Z. Tulipánt, A. Kardos, and G. Somogyi, Eur. Phys. J. C **77**, 749 (2017), arXiv:1708.04093 [hep-ph].

[17] I. Moult and H. X. Zhu, JHEP **08**, 160 (2018), arXiv:1801.02627 [hep-ph].

[18] I. Moult, G. Vita, and K. Yan, JHEP **07**, 005 (2020), arXiv:1912.02188 [hep-ph].

[19] M. A. Ebert, B. Mistlberger, and G. Vita, JHEP **08**, 022 (2021), arXiv:2012.07859 [hep-ph].

[20] I. Moult, H. X. Zhu, and Y. J. Zhu, (2022), arXiv:2205.02249 [hep-ph].

[21] C. Duhr, B. Mistlberger, and G. Vita, (2022), arXiv:2205.02242 [hep-ph].

[22] H. Chen, M.-X. Luo, I. Moult, T.-Z. Yang, X. Zhang, and H. X. Zhu, JHEP **08**, 028 (2020), arXiv:1912.11050 [hep-ph].

[23] H. Chen, I. Moult, X. Zhang, and H. X. Zhu, Phys. Rev. D **102**, 054012 (2020), arXiv:2004.11381 [hep-ph].

[24] K. Yan and X. Zhang, Phys. Rev. Lett. **129**, 021602 (2022), arXiv:2203.04349 [hep-th].

[25] T.-Z. Yang and X. Zhang, JHEP **09**, 006 (2022), arXiv:2208.01051 [hep-ph].

[26] T.-Z. Yang and X. Zhang, Phys. Rev. D **109**, 114036 (2024), arXiv:2402.05174 [hep-ph].

[27] D. Chicherin, I. Moult, E. Sokatchev, K. Yan, and Y. Zhu, Phys. Rev. D **110**, L091901 (2024), arXiv:2401.06463 [hep-th].

[28] R. Ma, J. Gong, J. Lin, K. Yan, G. Yang, and Y. Zhang, JHEP **02**, 025 (2026), arXiv:2506.02061 [hep-ph].

[29] A. Sabry, Nucl. Phys. **33**, 401 (1962).

[30] D. J. Broadhurst, J. Fleischer, and O. V. Tarasov, Z. Phys. C **60**, 287 (1993), arXiv:hep-ph/9304303.

[31] S. Laporta and E. Remiddi, Nucl. Phys. B **704**, 349 (2005), arXiv:hep-ph/0406160.

[32] S. Bloch and P. Vanhove, J. Number Theor. **148**, 328 (2015), arXiv:1309.5865 [hep-th].

[33] L. Adams, C. Bogner, and S. Weinzierl, J. Math. Phys. **54**, 052303 (2013), arXiv:1302.7004 [hep-ph].

[34] A. B. Goncharov, M. Spradlin, C. Vergu, and A. Volovich, Phys. Rev. Lett. **105**, 151605 (2010), arXiv:1006.5703 [hep-th].

[35] C. W. Bauer, A. Frink, and R. Kreckel, J. Symb. Comput. **33**, 1 (2002), arXiv:cs/0004015 [cs.SC].

[36] L. Naterop, A. Signer, and Y. Ulrich, Comput. Phys. Commun. **253**, 107165 (2020), arXiv:1909.01656 [hep-ph].

[37] Y. Wang, L. L. Yang, and B. Zhou, (2021), arXiv:2112.04122 [hep-ph].

[38] M. Walden and S. Weinzierl, Comput. Phys. Commun. **265**, 108020 (2021), arXiv:2010.05271 [hep-ph].

[39] C. Duhr, F. Lorkowski, R. Marzucca, S. Mauc, and S. Weinzierl, (2026), arXiv:2602.09956 [hep-ph].

[40] L. J. Dixon, J. Drummond, T. Harrington, A. J. McLeod, G. Papathanasiou, and M. Spradlin, JHEP **02**, 137 (2017), arXiv:1612.08976 [hep-th].

[41] S. Caron-Huot, L. J. Dixon, A. McLeod, and M. von Hippel, Phys. Rev. Lett. **117**, 241601 (2016), arXiv:1609.00669 [hep-th].

[42] S. Caron-Huot, L. J. Dixon, F. Dulat, M. von Hippel, A. J. McLeod, and G. Papathanasiou, JHEP **08**, 016 (2019), arXiv:1903.10890 [hep-th].

[43] L. J. Dixon, A. J. McLeod, and M. Wilhelm, JHEP **04**, 147 (2021), arXiv:2012.12286 [hep-th].

[44] L. J. Dixon, O. Gurdogan, A. J. McLeod, and M. Wilhelm, JHEP **07**, 153 (2022), arXiv:2204.11901 [hep-th].

[45] B. Basso, L. J. Dixon, and A. G. Tumanov, JHEP **02**, 034 (2025), arXiv:2410.22402 [hep-th].

[46] T. Cai, G. W. Merz, F. Charton, N. Nolte, M. Wilhelm, K. Cranmer, and L. J. Dixon, Mach. Learn. Sci. Tech. **5**, 035073 (2024), arXiv:2405.06107 [cs.LG].

[47] T. Cai, F. Charton, K. Cranmer, L. J. Dixon, G. W. Merz, and M. Wilhelm, JHEP **04**, 143 (2025), arXiv:2501.05743 [hep-th].

[48] Y. Guo, L. Wang, and G. Yang, Phys. Rev. Lett. **127**, 151602 (2021), arXiv:2106.01374 [hep-th].

[49] A. Dersy, M. D. Schwartz, and X. Zhang, Int. J. Data Sci. Math. Sci. **1**, 135 (2024), arXiv:2206.04115 [cs.LG].

[50] D. Chicherin, J. Henn, and V. Mitev, JHEP **05**, 164 (2018), arXiv:1712.09610 [hep-th].

[51] S. Caron-Huot, L. J. Dixon, M. von Hippel, A. J. McLeod, and G. Papathanasiou, JHEP **07**, 170 (2018), arXiv:1806.01361 [hep-th].

[52] J. Henn, E. Herrmann, and J. Parra-Martinez, JHEP **10**, 059 (2018), arXiv:1806.06072 [hep-th].

[53] S. He, Z. Li, and Q. Yang, JHEP **12**, 110 (2021), [Erratum: JHEP 05, 075 (2022)], arXiv:2106.09314 [hep-th].

[54] S. He, Z. Li, and Q. Yang, JHEP **06**, 067 (2026), arXiv:2112.11842 [hep-th].

[55] O. Barrera, A. Dersy, R. Husain, M. D. Schwartz, and X. Zhang, (2025), arXiv:2507.17815 [hep-th].

[56] R. Morales, A. Spiering, M. Wilhelm, Q. Yang, and C. Zhang, Phys. Rev. Lett. **131**, 041601 (2023), arXiv:2212.09762 [hep-th].

[57] F. Brown, Commun. Num. Theor. Phys. **11**, 453 (2017), arXiv:1512.06409 [math-ph].

[58] L. Adams and S. Weinzierl, Commun. Num. Theor. Phys. **12**, 193 (2018), arXiv:1704.08895.

[59] L. Adams and S. Weinzierl, Phys. Lett. B **781**, 270 (2018), arXiv:1802.05020 [hep-ph].

[60] C. Bogner, A. Schweitzer, and S. Weinzierl, Nucl. Phys. B **922**, 528 (2017), arXiv:1705.08952 [hep-ph].

[61] J. Broedel, C. Duhr, F. Dulat, and L. Tancredi, JHEP **05**, 093 (2018), arXiv:1712.07089 [hep-th].

[62] G. F. Sterman, ILL-TH-75-32 (1975).

[63] N. A. Sveshnikov and F. V. Tkachov, Phys. Lett. B **382**, 403 (1996), arXiv:hep-ph/9512370.

[64] F. V. Tkachov, Int. J. Mod. Phys. A **12**, 5411 (1997), arXiv:hep-ph/9601308.

[65] G. P. Korchemsky and G. F. Sterman, Nucl. Phys. B **555**, 335 (1999), arXiv:hep-ph/9902341.

[66] E. Remiddi and J. A. M. Vermaseren, Int. J. Mod. Phys. A **15**, 725 (2000), arXiv:hep-ph/9905237.

[67] H. Cheng and T. T. Wu, *Expanding Protons: Scattering at High Energies* (MIT Press, Cambridge, MA, 1987).

[68] S. Müller-Stach, S. Weinzierl, and R. Zayadeh, Commun. Num. Theor. Phys. **6**, 203 (2012), arXiv:1112.4360 [hep-ph].

[69] E. Panzer, Comput. Phys. Commun. **188**, 148 (2015), arXiv:1403.3385 [hep-th].

[70] J. Franel, L'Intermédiaire des Mathématiciens **1**, 45 (1894).

[71] D. Zagier, in *Groups and Symmetries: From Neolithic Scots to John McKay*, CRM Proceedings and Lecture Notes, Vol. 47 (American Mathematical Society, Providence, RI, 2009) pp. 349–366.

[72] D. Maitre, Comput. Phys. Commun. **174**, 222 (2006), arXiv:hep-ph/0507152.

[73] C. Duhr and F. Dulat, JHEP **08**, 135 (2019), arXiv:1904.07279 [hep-th].

[74] H. S. Hannesdottir, A. J. McLeod, M. D. Schwartz, and C. Vergu, Phys. Rev. D **111**, 085003 (2025), arXiv:2410.02424 [hep-ph].

[75] J. Gong, A. Pokraka, K. Yan, and X. Zhang, (2025), arXiv:2509.22782 [hep-th].

[76] C. Fevola, S. Mizera, and S. Telen, Comput. Phys. Commun. **303**, 109278 (2024), arXiv:2311.16219 [math-ph].

[77] M. Correia, M. Giroux, and S. Mizera, Comput. Phys. Commun. **320**, 109970 (2026), arXiv:2503.16601 [hep-th].

[78] H. Chen, X. Zhou, and H. X. Zhu, (2023), arXiv:2301.03616 [hep-th].

[79] K. Ryan and N. Heninger, in *Advances in Cryptology – CRYPTO 2023*, Lecture Notes in Computer Science (Springer, 2023) pp. 3–36, cryptology ePrint Archive 2023/237.

[80] F. V. Tkachov, Phys. Lett. B **100**, 65 (1981).

[81] K. G. Chetyrkin and F. V. Tkachov, Nucl. Phys. B **192**, 159 (1981).

[82] S. Laporta, Int. J. Mod. Phys. A **15**, 5087 (2000), arXiv:hep-ph/0102033.

[83] A. V. Kotikov, Phys. Lett. B **254**, 158 (1991).

[84] E. Remiddi, Nuovo Cim. A **110**, 1435 (1997), arXiv:hep-th/9711188.

[85] T. Gehrmann and E. Remiddi, Nucl. Phys. B **580**, 485 (2000), arXiv:hep-ph/9912329.

[86] J. M. Henn, Phys. Rev. Lett. **110**, 251601 (2013), arXiv:1304.1806.

[87] A. B. Goncharov, Math. Res. Lett. **5**, 497 (1998), arXiv:1105.2076 [math.AG].

[88] F. C. S. Brown, Commun. Math. Phys. **287**, 925 (2009), arXiv:0804.1660 [math.AG].